On the impact of VR assessment on the Quality of Experience of Highly Realistic Digital Humans

A Volumetric Video Case Study

Irene Viola · **Shishir Subramanyam** · **Jie Li** · **Pablo Cesar**

Abstract Fuelled by the increase in popularity of virtual and augmented reality applications, point clouds have emerged as a popular 3D format for acquisition and rendering of digital humans, thanks to their versatility and real-time capabilities. Due to technological constraints and real-time rendering limitations, however, the visual quality of dynamic point cloud contents is seldom evaluated using virtual and augmented reality devices, instead relying on prerecorded videos displayed on conventional 2D screens. In this study, we evaluate how the visual quality of point clouds representing digital humans is affected by compression distortions. In particular, we compare three different viewing conditions based on the degrees of freedom that are granted to the viewer: passive viewing (2DTV), head rotation (3DoF), and rotation and translation (6DoF), to understand how interacting in the virtual space affects the perception of quality. We provide both quantitative and qualitative results of our evaluation involving 78 participants, and we make the data publicly available. To the best of our knowledge, this is the first study evaluating the quality of dynamic point clouds in virtual reality, and comparing it to traditional viewing settings. Results highlight the dependency of visual quality on the content under test, and limitations in the way current data sets are used to evaluate compression solutions. Moreover, influencing factors in quality evaluation in VR, and shortcomings in how point cloud encoding solutions handle visually-lossless compression, are discussed.

1 Introduction

Recent technological advances in devices for capturing and rendering immersive media contents, together with the fast processing capabilities of commodity hardware, have fostered the development of new applications for Virtual Reality (VR), Augmented Reality (AR) and Mixed Reality (XR). Such applications usher a new way to engage and interact with media contents: whereas in traditional 2D consumption, users are passive receivers and have limited possibilities of manipulating the contents they are visualizing, immersive media allow for more interactivity in deciding which content should be displayed by each user. Commonly, immersive media applications can be classified based on the Degrees of Freedom (DoF) that are available to the end user to explore the virtual world: 3DoF refers to the availability of only head rotation as a tool for interaction, as for example in omnidirectional imagining, whereas 6DoF refers to the ability to operate translational movements as well as rotational movements in the 3D space.

In order to populate immersive VR, AR and XR applications, volumetric contents are needed. In this context, point clouds have emerged as a popular format to capture and represent volumetric reconstructions of real-world objects and people, due to their simplicity and versatility. Geometrical representation in point clouds is obtained through a collection of points with x, y and z coordinates in Euclidean space; in addition, attributes such as colour may be included included at each point location. This enables a simple representation

Irene Viola and Jie Li
CWI, Amsterdam, The Netherlands
E-mail: irene@cwi.nl, jie.li@cwi.nl
Shishir Subramanyam and Pablo Cesar
CWI, Amsterdam, and TU Delft, Delft, The Netherlands
E-mail: subraman@cwi.nl, p.s.cesar@cwi.nl

that requires no additional pre-processing, is resilient to noise introduced during capture, and enforces no restrictions on the attributes that can be encoded at each point location. However, one main drawback for the deployment of this type of content is the large amount of data that is required in order to produce a photorealistic representation: uncompressed, a single point cloud frame containing one million points requires roughly 20MB to be transmitted. Compression becomes therefore essential for efficient storage and feasible transmission over bandwidth-limited networks. Thus, significant research [34] and industrial [43] effort has been focused on optimizing encoding and transmission, as demonstrated by the ongoing standardization endeavors by bodies such as JPEG [14, 44] and MPEG [27].

Given the significant storage and bandwidth requirements for dense dynamic point clouds, decisions need to be taken regarding the delivery (type of encoder, bit-rate) to ensure an acceptable quality of experience, depending on the viewing conditions. In a previous paper [45], we analysed the impact of different viewing conditions in VR environments, namely, with 3DoF or 6DoF locomotion. With this work, we aim to extend our previous analysis by including results and discussions obtained in a baseline viewing condition using traditional 2D screens (2DTV), which is by large the most commonly used environment for user studies for point cloud quality assessment.

In this paper, we report findings obtained in a user study involving 78 participants assessing 72 stimuli based on eight dynamic point clouds sequences depicting humans. Each point cloud sequence was compressed using two encoding solutions at 4 bit-rates, and evaluated in three viewing conditions (6DoF, 3DoF and 2DTV). The gathered data include rating scores, presence questionnaires, simulator sickness reports, along with average watching time. Contributions of the paper are three-fold:

1. An extensive evaluation of the quality of highly realistic digital humans represented as dynamic point clouds in immersive and traditional TV viewing conditions is provided. Existing protocols [4, 6, 7, 52, 56] did not consider the dynamic nature of the point clouds, focused on one type of data set, did not take into account VR viewing conditions, and did not compare VR findings with 2DTV conditions using dynamic contents;

2. Quantitative subjective results about the perceived quality of the contents, along with qualitative insights on what is important for users in interacting with digital humans in VR, are presented. Such results will help in better configuring the network conditions for the delivery of points clouds for real-time transmission, and have implications over ongoing research and standardisation work regarding the underlying compression technology;

3. The collected raw data, which is comprised of rating scores, presence questionnaires, and simulator sickness

reports, is made available to the research community, along with scripts to faithfully recreate the stimuli under exam[1]. This will aid reproducibility, while contributing to ongoing research in the area.

The remainder of the paper is organised as follows. Section 2 summarises the related work in the field of point cloud compression and subjective visual quality assessment. Section 3 details the methodology that was followed to conduct the experiments and analyse the data. In Section 4, we report the quantitative and qualitative results of the subjective visual quality assessment, along with commenting the findings in terms of simulator sickness, presence, and interaction time. Key factors and issues for visual quality assessment of dynamic point clouds are discussed in Section 5. Finally, Section 6 concludes the paper. Additional data regarding the statistical analysis of the results is offered in Appendix 6.

2 Related work

2.1 Quality assessment for point clouds

There is a growing interest on subjective quality assessment of point clouds rendered on 2D displays. Zhang et al. [56] evaluated the quality degradation effect of resolution, shape and color on static point clouds. The results indicate that resolution is almost linearly correlated with the perceived quality, and color has less impact than shape on the perceived quality. Zerman et al. [52] compressed two dynamic human point clouds using a state-of-the-art algorithm [32], and assessed the effects of this algorithm and input point counts on the perceived quality. Their results showed that no direct correlation was found between human viewers' quality ratings and input point counts. In a recent study [44], a protocol to conduct subjective quality evaluations and benchmark objective quality metrics were proposed. The viewers passively assessed the quality of a set of static point clouds, as animations with pre-defined movement path. In a comprehensive work by Alexiou et al. [7], the entire set of emerging point cloud compression encoders developed in the MPEG committee were evaluated through a series of subjective quality assessment experiments. Nine static models, including both humans and objects, were used in the experiments. The experiments provided insights regarding the performance of the encoders and the types of degradation they introduce. Zerman et al. [54] compared the visual quality of point cloud and mesh contents compressed using state-of-the-art algorithms, concluding that, while meshes are more suitable for high bitrate streaming, point cloud compression appears to be more advantageous at lower bitrates. Perry et al. [37] conducted an experiment in 4 laboratories, comparing the latest standardized compression solutions on static point cloud contents.

---

[1] `https://github.com/cwi-dis/2DTV_VR_QoE`

(a) *V-PCC* (b) *MPEG Anchor*

Fig. 1: Point Cloud Digital Humans compressed using two point cloud codecs, V-PCC (left) and MPEG anchor (right), at the 4 selected bit-rates.

Only a limited number of point cloud quality assessment studies have been conducted in immersive environments. Mekuria et al. [34] evaluated the subjective quality of their codec performance in a realistic 3D tele-immersive system, in which users were represented as 3D avatars and/or 3D dynamic point clouds, and could navigate in the virtual space using mouse cursor in a desktop setting. Several aspects of quality, such as level of immersiveness, togetherness, realism, quality of motion, were considered. Alexiou and Ebrahimi [6] proposed the use of AR to subjectively evaluate the quality of colorless point cloud geometry. Zerman et al. [53] presented a behaviour analysis of users interacting with colored volumetric media in a AR application. Tran et al. [48] suggested that, in case of evaluating video quality in an immersive setup, aspects such as cybersickness and presence should not be overlooked. Recently, an evaluation of static point cloud contents was conducted in a VR environment [9].

Our work aims at comparing different viewing paradigms for dynamic point clouds, namely 6DoF, 3DoF, and 2DTV conditions. Such a comparison is largely absent in the literature, as previous work has mainly focused on static point cloud contents and single viewing conditions.

2.2 Point cloud compression

A single point cloud frame is represented by an unordered collection of points sampled from the surface of an object. In a dynamic sequence of point clouds, there are no correspondences of points maintained across frames. Thus, detecting spatial and temporal redundancies is often difficult, making point cloud compression challenging. Octrees have been used extensively as a space partitioning structure to represent point cloud geometry [26, 33]. They are a 3D extension of the 2D quadtree used to encode video and images.

Research into point cloud compression can be broadly divided into two categories: model-based and projection-based. The first uses signal processing or deep learning techniques to compress either the geometrical composition of the point cloud, or its attributes, such as color. Zhang et al. [55] pro-posed a method to compress point cloud attributes using a Graph Fourier Transform. They assume that an octree has been created and separately coded for geometry prior to coding attributes. De Queiroz and Chou [40] used a Region Adaptive Hierarchical Transform (RAHT) to use the colors of nodes in lower levels of the octree to predict the colors of nodes in the next level. In [11], authors adopt techniques from traditional image and video processing, using 3D block prediction in combination with shape-adaptive DCT and graph transforms.

The second category of point cloud codecs aim at projecting the point cloud information onto a 2D canvas, subsequently using legacy image and video compression solutions to encode them. Intra Frame coding in octrees can be achieved by entropy coding the occupancy codes, and then compress the color attributes by mapping them to a 2D grid and using legacy JPEG image compression, as shown in [34]. In 2017, MPEG started a standardization activity to determine a new standard codec for point clouds. They used the codec created by Mekuria et al. [34] as an anchor to evaluate proposals. To encode dynamic point cloud sequences, MPEG has currently standardized one method for dynamic dense point clouds, namely V-PCC [22], and is in the process of standardizing one method for dynamically acquired, sparse point clouds, namely G-PCC [21].

Recently, deep learning solutions for point cloud compressions have been proposed, to encode either geometry or color information, or a combination thereof. Quach et al. [38] propose the use of an auto-encoder to efficiently compress geometry information, and they subsequently analyse the impact of several parameters on the performance [39]. Similarly, Guarda et al. [18] propose a Convolutional Neural Network (CNN) architecture to encode and decode point cloud contents. They further analyse its performance in [17], and extend the work in [19] by employing explicit and implicit quantization. A deeper architecture is proposed in [50], which uses 3D convolutional layers along with variational auto-encoders to achieve favorable compression efficiency. In [5], Alexiou et al. propose a deep learning architecture to encode both geometry and color attributes, and analyse the

performance of various parameters on the coding efficiency and visual quality.

A complete survey of point cloud compression solutions can be found here [10]. In our work, we elected to adopt the MPEG Anchor that was used to evaluate the Call for Proposals for the MPEG standardization efforts in point cloud compression [43], and the MPEG standard for dynamic point clouds V-PCC [22], as they have both been widely used in quality evaluation campaigns in the literature.

3 Methodology

3.1 Dataset Preparation

A dataset of dynamic point cloud sequences was used from the MPEG repository. All sequences were clipped to five seconds and sampled at 30 frames per second. This included point cloud sequences [12] captured using photogrammetry (*Longdress, Loot, Red and black, Soldier*, shown in figure 2) and one sequence of a synthetic character sampled from an animated mesh (*Queen*). Four additional point cloud sequences; *Manfred, Despoina, Sarge* (shown in Figure 2) were added for the evaluation. These sequences were created using motion-captured animated mesh sequences.

Keyframes were selected at 30 frames per second and extracted along with the associated mesh materials. Particular care was put in ensuring the selected sequences have the characters facing the user and speaking in their general direction. Then, 1 million points were randomly sampled, independently per key frame to create a consistent groundtruth dataset. The points were sampled from the mesh surface with a probability proportional to the area of the underlying mesh face. This was done to ensure no direct point correspondences across point cloud frames, to mimic realistic acquisition and maintain consistency with the rest of the dataset. The X, Y, Z coordinates of each point was represented using an unsigned integer, as is required for the current version of the V-PCC software. Texture information was encoded as 8-bit RGB.

The contents were compressed using two widely available codecs: the MPEG V-PCC codec in the Release 7.0 [43] (*C1*), as the state-of-the-art solution in point cloud compression, and the MPEG anchor codec [34] (*C2*), as a baseline release with real-time capabilities. Bitrate points were selected based on the provided presets for *C1*, to ensure fair use. For the additional point cloud sequences for which no configuration file was available, the one provided by MPEG for the *Queen* sequence was used for all the contents. We selected the rate points 1, 3 and 5 from the provided preset V-PCC configurations and extended it with an additional final rate point using a texture Quantization Parameter (QP) of 8, a geometry QP of 12, and an occupancy precision of 2. We re-label the rate points as R1, R2, R3 and R4, respectively. All sequences are encoded using the C2AI (Category 2 All Intra) config. For the photogrammetry sequences, we use the predefined dedicated configuration files for each sequence, at the same rate points.

C2 is used in an all-intra configuration to match the bitrates per sequence and rate point (R1-R4) with a tolerance of 10%, as defined in the MPEG call for proposals. We use an octree depth from 7 to 10 for the rate points R1 to R4, respectively. The highest possible JPEG quantization parameter values were then chosen per sequence, while meeting the target bit rate set using *C1*. An example of content *Loot* encoded with the two compression solutions at the selected rate points is shown in Figure 1.

3.2 Experiment setup

All point cloud sequences were rendered using the Unity game engine, by storing all the points of each frame in a vertex buffer, and then drawing procedural geometry on the GPU. The point clouds were rendered using a quadrilateral at each point location with a fixed offset of 0.08 units (this corresponds to a side length of approximately 2mm) around each point (placed at the centre) for all the sequences, to be consistent. In the case of bitrate R1 generated using the MPEG anchor, we increased the offset value to 0.16 by eye, as the resulting point clouds were too sparse (shown in Figure 1b). We maintain a fixed frame rate of 30fps throughout the experiment.

Three viewing conditions were selected for comparison: 6DoF, 3DoF, and 2DTV condition. For the 6DoF and 3DoF viewing conditions, participants were asked to wear an Oculus Rift CV1 HMD to view each of the point cloud sequences. For the 3DoF condition, participants were asked to sit on a swivel chair placed at a fixed location in the room and navigate using head movements alone, whereas for the 6DoF condition, participants were allowed to navigate freely within the room. Each sequence was 5 seconds long, after which the playback looped around. We set the background of the virtual room to mid-grey, to avoid distractions. The Oculus Guardian System was used to display in-application wall and floor markers if the participants got too close to the boundary. We used a workstation with 2 GeForce GTX 1080 Ti in SLI for the GPU and an Intel Core i9 Skylake-X 2.9GHz CPU. For the 2DTV condition, the videos were created offline, using the same rendering as the other two viewing condition, and played back to the users using MPV[2]. A 25" Dell UltraSharp U2515H QHD (2560x1440 px) monitor was used to display the videos. The monitor was calibrated using an i1Display Pro color calibration device according to the following profile: sRGB Gamut, D65 white point, 120cd/m2 brightness, and minimum black level of 0.2 cd/m2. The test was performed in a room with controlled lighting and mid-grey

---

[2] https://mpv.io/

Fig. 2: Sequences used for the test, from left to right: Manfred, Sarge, Despoina, Queen, Longdress, Loot, Red and black, Soldier

walls, in accordance with ITU-T Recommendation BT.500-13 [23].The illumination level measured on the screens was 15 lux.

3.3 Subjective methodology

To perform the experiments, the subjective methodology Absolute Category Rating with Hidden References (ACR-HR) was selected, according to ITU-T Recommendations P.910 [24]. Participants were asked to observe the video sequences depicting digital humans, and rate the corresponding visual quality on a scale from 1 to 5 (*1-Bad*, *2-Poor*, *3-Fair*, *4-Good*, and *5-Excellent*).

A series of pilot studies were conducted to determine the positioning of digital humans in the virtual space and the length of each sequence, to ensure the sequences were running smoothly within the limited computer RAM. Due to the huge size of the test material, it was not possible to evaluate all 8 point cloud contents in one single session, as long loading times would have brought fatigue to the participants and corrupted the results. Thus, we decided to split the evaluation into two separate tests: one focused on the evaluation of contents obtained from random sampling of meshes (**T1**: contents *Queen*, *Manfred*, *Despoina* and *Sarge*), and one focused on contents acquired through photogrammetry (**T2**: contents *Long dress*, *Soldier*, *Red and black*, and *Loot*). From each sequence, a subset of frames comprising 5 seconds was selected.

Before the test took place, 3 training sequences depicting examples of *1-Bad*, *5-Excellent* and *3-Fair* were shown to the users to help them familiarize with the viewing condition and test setup, and to guide their rating. Following ITU-T Recommendation BT.500-13 [23], the training sequences were created using one additional content not shown during the test, to prevent biased results. Each content sequence was encoded using the point cloud compression algorithms under test.

For each test and viewing condition, 36 stimuli were evaluated. For each stimulus, the 5 second sequence was played at least once in full, and kept in loop until the participants gave their score. The order of the displayed stimuli was randomized per participant and per viewing condition, and the same content was never displayed twice in a row to avoid bias. Moreover, the presentation order of viewing conditions was randomized between participants, to prevent any confounding effect. Two dummy samples were added at the beginning of each viewing session to ease participants into the task, and the corresponding scores were subsequently discarded.

After each VR viewing conditions (6DoF and 3DoF), participants were requested to fill in the Igroup Presence Questionnaire (IPQ) [42] on a 1-7 discrete scale (1=fully disagree to 7=totally agree) and Simulator Sickness Questionnaire (SSQ) on a 1-4 discrete scale (1=none to 4=severe) [29]. IPQ has three subscales, namely Spatial Presence (SP), Involvement (INV) and Experienced Realism (REAL), and one additional general item (G) not belonging to a subscale, which assesses the general "sense of being there", and has high loadings on all three factors, with an especially strong loading on SP [42]. SSQ was developed to measure cybersickness in computer simulation and was derived from a measure of motion sickness [29]. For both T1 and T2, after the two viewing conditions, participants were interviewed to 1) compare their experiences of assessing quality in 3DoF and 6DoF, and 2) reflect on the factors they considered when assessing the quality.

For the 6DoF and 3DoF viewing conditions, a total of 27 participants were recruited for T1 (12 males, 15 female, average age: 22,48 years old), whereas 25 participants were recruited for T2 (17 males, 8 females, average age: 28,39 years old). The 2DTV viewing condition was conducted separately, with 26 participants for both T1 and T2 (17 males, 9 females, average age: 34,76 years old). All participants were screened for color vision and visual acuity, using Isihara and Snellen charts, respectively, according to ITU-T Recommendations P.910 [24].

3.4 Data analysis

Outlier detection was performed separately for each of the test datasets T1 and T2, following ITU-T Recommendations

P.913 [25]. The recommended threshold values of $r_1 = 0.75$ and $r_2 = 0.8$ were used. One outlier was found in test dataset T1, and the corresponding scores were discarded. No outliers were found in the scores collected for T2. Since the 2DTV viewing condition was tested with a different subject population, outlier detection was conducted separately. No outlier was detected for this viewing condition.

After outlier detection, the Mean Opinion Score (MOS) was computed for each stimulus, independently per viewing condition. The associated 95% Confidence Intervals (CIs) were obtained assuming a Student's t-distribution. Additionally, the Differential MOS (DMOS) was obtained by applying HR removal, following the procedure described in ITU-T Recommendations P.913 [25]. Non-parametric statistical analysis was then used to analyze if there are statistical differences among variables, using the MATLAB Statistics and Machine Learning Toolbox, along with the ARTool package in R [15, 28].

4 Results

4.1 Subjective quality assessment

Figures 3 and 4 shows the results of the subjective quality assessment of the contents comprising test T1 and test T2, for the 6DoF, 3DoF and 2DTV viewing conditions. In particular, the DMOS scores associated with the compressed contents are shown with solid lines, along with relative CIs, whereas the dashed lines represent the respective HR scores with the corresponding confidence intervals.

To assess whether significant differences could be found between the three viewing conditions under test, we ran a non-parametric Kruskal-Wallis test, separately for test T1 and T2. The test was chosen as the gathered data was not found to be normally distributed, according to the Shapiro-Wilk normality test (T1: $W = 0.906$, $p < .001$; T2: $W = 0.909$, $p < .001$). We found a significant effect of the viewing condition on the scores for test T1 ($\chi^2 = 37.56$, $p < .001$). Post-hoc analysis using Mann-Whitney U test with Bonferroni correction ($\alpha = .05/3$) revealed significant differences between 6DoF and 2DTV viewing conditions ($p < .001$, $r = 0.09$), and between 3DoF and 2DTV viewing conditions ($p < .001$, $r = 0.14$), but not between 6DoF and 3DoF ($p = 0.101$, $r = 0.04$). Values seem to indicate an effect of VR viewing condition with respect to traditional TV viewing on the final scores; however, the effect sizes suggest that, if the effect indeed exists, it is small. For test T2, no significant effect was found for viewing condition on the scores ($\chi^2 = 5.19$, $p = 0.075$).

It can be observed that codec *C1* has generally a more favorable performance with respect to *C2*. This is especially evident for the contents acquired through photogrammetry (see Fig. 4), for which the gap among the two codecs is

Table 1: Pairwise post-hoc test on the contents for test T1 and T2, using Wilcoxon signed-rank test with Bonferroni correction.

		Z	p	r
T1	*Manfred - Sarge*	-1.10	0.270	0.03
	Manfred - Despoina	-1.59	0.111	0.04
	Manfred - Queen	5.57	<.001	0.15
	Sarge - Despoina	-0.54	0.588	0.01
	Sarge - Queen	6.75	<.001	0.18
	Despoina - Queen	7.04	<.001	0.19
T2	*Long dress - Loot*	-5.19	<.001	0.14
	Long dress - Red and black	-0.05	0.960	0.00
	Long dress - Soldier	-2.73	0.006	0.07
	Loot - Red and black	4.99	<.001	0.14
	Loot - Soldier	2.08	0.037	0.06
	Red and black - Soldier	-2.61	0.009	0.07

more pronounced. Mann-Whitney U test confirmed statistical significance for the two codecs (T1: $Z = 6.60$, $p < .001$, T2: $Z = 22.06$, $p < .001$), albeit with notably different effect sizes between test T1 and T2 ($r = 0.13$ and $r = 0.45$, respectively).

A Kruskal-Wallis test performed on the scores revealed a significant effect of the content on the final scores, for both sets of contents (T1: $\chi^2 = 64.91$, $p < .001$, T2: $\chi^2 = 35.23$, $p < .001$). Table 1 shows the results of the post-hoc test conducted using Mann-Whitney U test with Bonferroni correction ($\alpha = .05/6$). Contents *Manfred, Sarge* and *Despoina* all show statistical significance with respect to content Queen ($p < .001$, $r \geq 0.15$ for all pairs). For contents acquired through photogrammetry, statistical significance was found between contents *Longdress* and *Loot*, and *Loot* and *Red and black* ($p < .001$, $r = 0.14$ in both cases), as well as between contents *Long dress* and *Soldier* ($p = 0.006$, $r = 0.07$). Results suggests that contents Long dress and Red and black appear to be given different scores with respect to contents Loot and Soldier. However, the effect sizes suggest that the effect, if existent, is quite small.

We also ran a Kruskal-Wallis test on the scores to assess whether the selected bit-rates were showing statistical significance. Results confirmed that the bit-rates have a significant effect for both tests (T1: $\chi^2 = 1164.14$, $p < .001$, T2: $\chi^2 = 1008.42$, $p < .001$). Post-hoc analysis using Mann-Whitney U test with Bonferroni correction ($\alpha = .05/6$), shown in Table 2 further confirmed that all pairwise comparisons were statistically significant, for both test T1 and T2 ($p < .001$, $r > 0.20$ for all pairs).

4.2 Data analysis

4.2.1 T1

In order to further analyze the effect of DoF conditions, contents, codecs and bit-rates, and relative interactions, on the
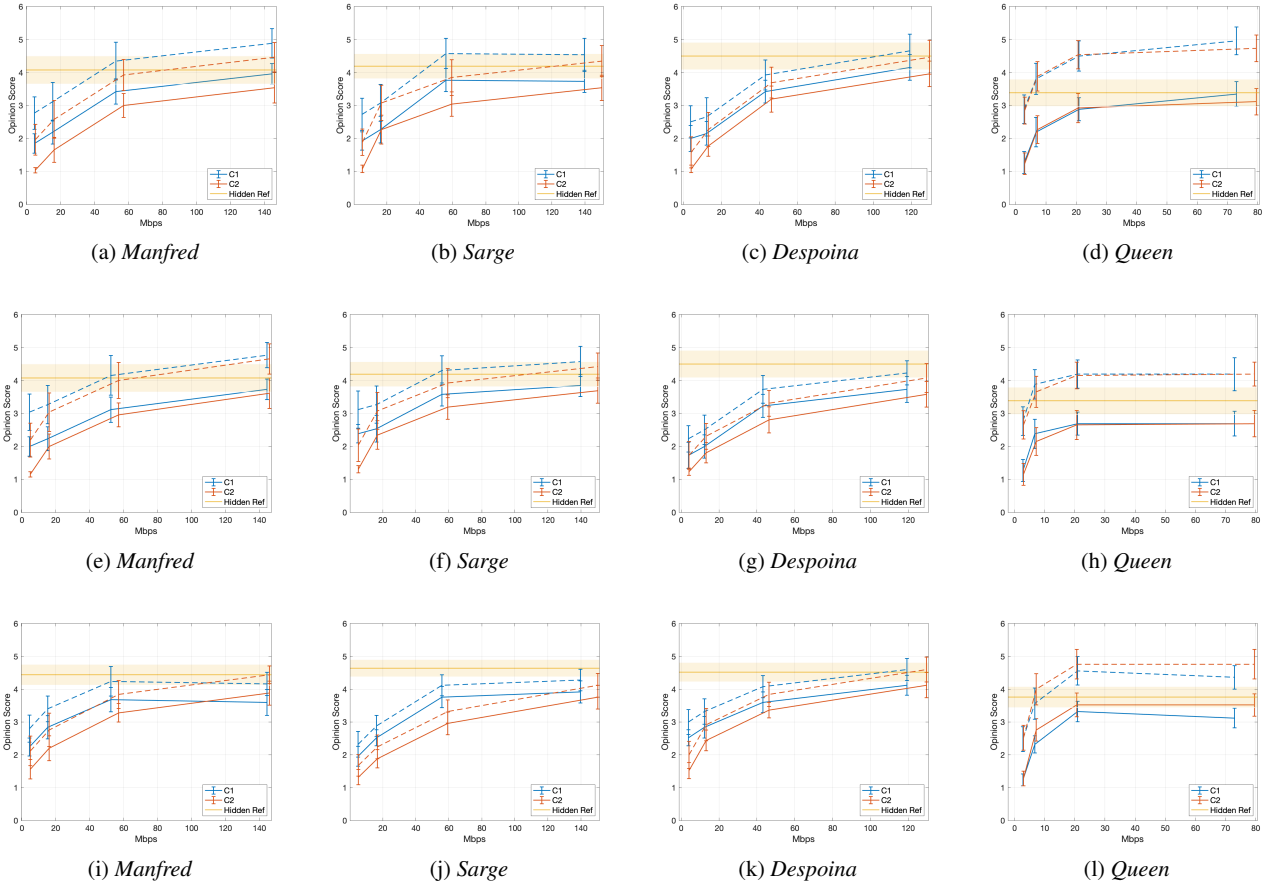
Fig. 3: DMOS against achieved bit-rate. HR scores are shown using a dashed plot. Each column represents a content in test T1, whereas the rows depict results obtained using the viewing conditions 6DoF, 3DoF and 2DTV, respectively.

Table 2: Pairwise post-hoc test on the bitrates for test T1 and T2, using Wilcoxon signed-rank test with Bonferroni correction.

		Z	p	r
T1	R1 - R2	-14.30	<.001	0.41
	R1 - R3	-25.54	<.001	0.73
	R1 - R4	-27.36	<.001	0.78
	R2 - R3	-17.03	<.001	0.49
	R2 - R4	-21.05	<.001	0.60
	R3 - R4	-7.30	<.001	0.21
T2	R1 - R2	-14.61	<.001	0.42
	R1 - R3	-23.84	<.001	0.68
	R1 - R4	-27.39	<.001	0.79
	R2 - R3	-11.20	<.001	0.32
	R2 - R4	-17.95	<.001	0.51
	R3 - R4	-8.53	<.001	0.24

gathered scores, we fitted a full linear mixed-effects model on the data, accounting for randomness introduced by the participants. Due to the non-normality of our data, the aligned rank transform was applied prior to the fitting [51]. Since the transform is designed for a fully randomized test, it is not suitable for the scores collected during the test, as the HR addition makes the design matrix rank deficient. However, the transform can be applied to the differential scores used to obtain DMOS, as it follows a fully randomized design. Thus, it was decided to perform the analysis on the differential scores. Post-hoc contrast tests were performed using the ART-C tool [15].

For test T1, analysis of deviance on the full mixed-effects model showed significance for main effects Content ($F = 53.98$, $df = 3$, $p < .001$), Codec ($F = 65.19$, $df = 1$, $p < .001$) and bit-rate ($F = 595.38$, $df = 3$, $p < .001$), but not for DoF ($F = 0.07$, $df = 2$, $p = 0.936$). Moreover, significant interaction effects were found for *DoF - Content* ($F = 11.39$, $df = 6$, $p < .001$), *Content - Codec* ($F = 9.97$, $df = 3$, $p < .001$), *Content - bit-rate* ($F = 6.04$, $df = 9$, $p < .001$) and *Codec - bit-rate* ($F = 8.96$, $df = 3$, $p < .001$). No interaction effect beyond the first level was found to be significant. The full results of the analysis of deviance can be found in Table 3.

Post-hoc interaction analysis using ART-C revealed significant differences at 5% level in 3DoF for content pairs *Manfred - Queen* ($p < .001$), *Sarge - Queen* ($p < .001$) and *Despoina - Queen* ($p < .001$); in 6DoF, for content pairs *Man-*

(a) *Long dress* (b) *Loot* (c) *Red and black* (d) *Soldier*

(e) *Long dress* (f) *Loot* (g) *Red and black* (h) *Soldier*

(i) *Long dress* (j) *Loot* (k) *Red and black* (l) *Soldier*
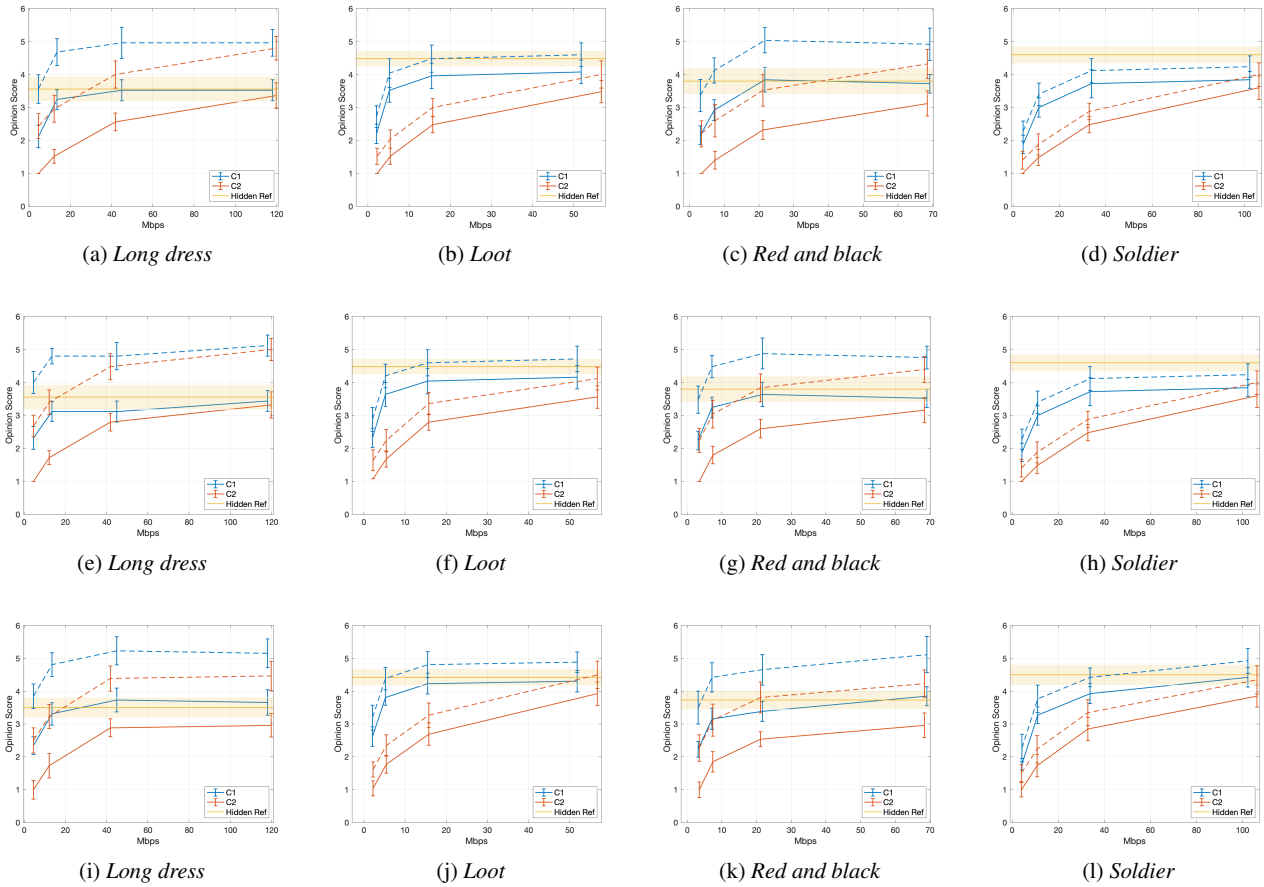
Fig. 4: DMOS against achieved bit-rate. HR scores are shown using a dashed plot. Each column represents a content in test T2, whereas the rows depict results obtained using the viewing conditions 6DoF, 3DoF and 2DTV, respectively.

Table 3: Analysis of deviance on the full mixed-effects model, for test T1.

	F	df	p
DoF	0.07	2	0.936
Content	53.98	3	$< .001$
Codec	65.19	1	$< .001$
Bitrate	595.38	3	$< .001$
DoF: Content	11.39	6	$< .001$
DoF: Codec	0.58	2	0.660
Content: Codec	9.97	3	$< .001$
DoF: Bitrate	1.70	6	0.116
Content: Bitrate	6.04	9	$< .001$
Codec: Bitrate	8.96	3	$< .001$
DoF: Content: Codec	0.71	6	0.643
DoF: Content: Bitrate	0.98	18	0.480
DoF: Codec: Bitrate	0.73	6	0.627
Content: Codec: Bitrate	1.23	9	0.273
DoF: Content: Codec: Bitrate	0.48	18	0.969

fred - Sarge ($p < .001$) and *Despoina - Queen* ($p < .001$); in the 2DTV condition, for content pairs *Manfred - Sarge* ($p = 0.019$) *Manfred - Queen* ($p < .001$), *Sarge - Despoina* ($p < .001$), *Sarge - Queen* ($p < .001$), and *Despoina - Queen*

($p = 0.024$). Additionally, several content pairs exhibited significant contrasts when different DoF were employed; for a full report of the contrasts, we invite readers to consult the appendix. Most notably, no significant effect was found when the same content was displayed in different DoF mediums; that is, for every content under exam, the pairs *3DoF - 6DoF*, *3DoF - 2DTV*, and *6DoF - 2DTV* were consistently above the 5% threshold of significance.

Regarding the interaction between factors Content and Codec, post-hoc analysis using ART-C showed significant differences at 5% level between the two codecs for all contents ($p < .001$) except *Queen*, for which the two codecs were deemed equivalent ($p = 0.995$). Furthermore, statistically significant differences were found, for *C1*, in content pairs *Manfred - Despoina* ($p = 0.006$), and *Despoina - Queen* ($p < .001$), and for *C2*, in content pairs *Manfred - Despoina* ($p = 0.010$), *Manfred - Queen* ($p < .001$), *Sarge - Queen* ($p < .001$), and *Despoina - Queen* ($p < .001$). Several content pairs were found to have significant contrasts when different codecs were employed; for a complete overview, we refer readers to the appendix.

Table 4: Analysis of deviance on the full mixed-effects model, for test T2.

	F	df	p
DoF	2.59	2	0.082
Content	165.56	3	< .001
Codec	1059.81	1	< .001
Bitrate	702.54	3	< .001
DoF: Content	1.99	6	0.064
DoF: Codec	1.08	2	0.340
Content: Codec	5.81	3	< .001
DoF: Bitrate	0.39	6	0.881
Content: Bitrate	6.30	9	< .001
Codec: Bitrate	44.89	3	< .001
DoF: Content: Codec	0.80	6	0.569
DoF: Content: Bitrate	1.10	18	0.341
DoF: Codec: Bitrate	1.12	6	0.346
Content: Codec: Bitrate	2.08	9	0.028
DoF: Content: Codec: Bitrate	0.69	18	0.820

Significant differences at 5% level were also found when considering post-hoc interactions between factors Content and Bitrate. In particular, the pair *Manfred - Queen* was found to have significant differences for rate *R2* ($p < .001$) and *R3* ($p = 0.018$); pair *Sarge - Queen* for rate *R1* ($p = 0.033$), *R2* ($p < .001$), and *R3* ($p = 0.005$); pair *Despoina - Queen*, for rate *R1* ($p < .001$), *R2* ($p < .001$), and *R3* ($p < .001$). No significant difference was found among contents at rate *R4*, indicating that, at the highest quality level, the contents were rated similarly. As expected, most of the comparisons between different bitrates, be it with the same or among different contents, yield statistically significant differences; the complete results are available in the appendix. Finally, results of the post-hoc analysis of interactions between factors Codec and Bitrate showed statistically significant differences at 5% level among the codecs for rate *R1* ($p < .001$) and *R3* ($p = 0.007$), but not for rate *R2* ($p = 0.052$ and *R4*) ($p = 0.986$). In the first case, the p-value is quite close to significance, whereas in the second, the test confirms our previous observations: at the highest quality level, the difference among codecs seems to be imperceptible. The rest of the combinations between codecs and bitrates lead to significant differences, with the exception of *C1-R3* versus *C2-R4* ($p = 0.054$), indicating that the null hypothesis cannot be rejected for *C2* at rate *R4* when compared to *C1* at rate *R3*; in other words, to achieve similar ratings to codec *C1* (MPEG V-PCC), codec *C2* (the MPEG anchor) requires higher bandwidth, which is in line with what observed in the previous section. More exhaustive results can be found in the appendix.

4.2.2 T2

Results of analysis of deviance on the full mixed-effects model for test T2 showed significance for main effects Content ($F = 165.56$, $df = 3$, $p < .001$), Codec ($F = 1059.81$, $df = 1$, $p < .001$) and Bitrate ($F = 702.54$, $df = 3$, $p < .001$) but not for DoF ($F = 2.59$, $df = 2$, $p = 0.0825$), similarly to what was seen for test T1. Two-way interactions were found significant at 5% level between Content and Codec ($F = 5.81$, $df = 3$, $p < .001$), Content and Bitrate ($F = 6.30$, $df = 9$, $p < .001$), and Codec and Bitrate ($F = 44.89$, $df = 3$, $p < .001$), as well as the three-way interaction between Content, Codec, and Bitrate ($F = 2.08$, $df = 9$, $p = 0.028$).

Post-hoc interaction analysis using ART-C for the three-way interaction between factors Content, Codec, and Bitrate revealed significant differences at 5% level between the two codecs under exam, when fixing content and bitrate level, for touples involving content *Longdress* at bitrate *R1* ($p < .001$), *R2* ($p < .001$), and *R3* ($p < .001$), but not for the highest bitrate *R4* ($p = 0.964$). Similarly, for content Soldier, touples had significant interactions at rate *R1* ($p = 0.010$), *R2* ($p < .001$), and *R3* ($p < .001$), but not *R4* ($p = 0.085$). For the other two contents, all touples at same bitrate were significant (*Loot, C1, R1 - Loot, C2, R1*: $p < .001$; *Loot, C1, R2 - Loot, C2, R2*: $p < .001$; *Loot, C1, R3 - Loot, C2, R3*: $p < .001$; *Loot, C1, R4 - Loot, C2, R4*: $p = 0.016$; *Red and black, C1, R1 - Red and black, C2, R1*: $p < .001$; *Red and black, C1, R2 - Red and black, C2, R2*: $p < .001$; *Red and black, C1, R3 - Red and black, C2, R3*: $p < .001$; *Red and black, C1, R4 - Red and black, C2, R4*: $p = 0.047$). This indicates that, with the exception of *Longdress* and *Soldier* at bitrate *R4*, for all rate points and all contents the two codecs were significantly different at 5% level.

Post-hoc interaction also revealed statistical difference among different contents: considering codec *C1* at bitrate *R1*, significant differences were found in content touples *Longdress - Loot* ($p < .001$), *Longdress - Soldier* ($p < .001$), *Loot - Soldier* ($p = 0.004$), and *Red and black - Soldier* ($p < .001$), but not for touples *Longdress - Red and black* ($p = 0.626$) and *Loot - Red and black* ($p = 0.091$); analogously, at bitrate *R2*, differences were found for touples *Longdress - Loot* ($p = 0.004$), *Longdress - Soldier* ($p < .001$), *Loot - Soldier* ($p < .001$), and *Red and black - Soldier* ($p < .001$), but not for touples *Longdress - Red and black* ($p = 0.198$) and *Loot - Red and black* ($p = 1$). At bitrate *R3*, significant differences were found only between touples *Longdress - Soldier* ($p < .001$); at bitrate *R4*, all content touples failed to reject the null hypothesis. This indicates that differences in DMOS scores among different contents are more prominent at lowest bitrates for codec *C1*, whereas for higher bitrates, contents received similar scores. When considering codec *C2*, at bitrate *R1*, significant differences were observed for content touples *Longdress - Loot* ($p < .001$), *Longdress - Soldier* ($p < .001$), *Loot - Red and black* ($p = 0.047$), and *Red and black - Soldier* ($p = 0.004$), but not for touples *Longdress - Red and black* ($p = 0.999$) and *Loot - Soldier* ($p = 1$); similarly, at bitrate *R2*, differences were deemed significant for content touples *Longdress - Loot* ($p < .001$),

Longdress - Soldier ($p <$ .001), *Loot - Red and black*, ($p <$ .001), and *Red and black - Soldier* ($p <$ .001), but not for *Longdress - Red and black* ($p = 0.994$) and *Loot - Soldier* ($p = 1$). This seems to indicate that, a lower bitrates, contents presenting the same gender were rated similarly. At bitrate *R3*, statistical difference could be observed among touples *Longdress - Loot* ($p <$ .001), *Longdress - Red and black* ($p = 0.018$), *Longdress - Soldier* ($p <$ .001), *Loot - Red and black* ($p = 0.009$), and *Red and black - Soldier* ($p <$ .001), but not for touple *Loot - Soldier* ($p = 1$), whereas for bitrate *R4*, statistical differences at a significant level were only observed between *Longdress - Soldier* ($p = 0.015$). Results indicate that for the highest bitrate, similar trends can be generally observed between different contents for both codecs under consideration, whereas as bitrate decreases, more differences can be spotted in DMOS trends.

Finally, post-hoc interaction analysis revealed significant differences at 5% level, for content *Longdress* encoded with codec *C1*, between bitrate *R1* with respect with all the other bitrates (*R1 - R2*: $p <$ .001; *R1 - R3*: $p <$ .001; *R1 - R4*: $p <$ .001); however, no significant difference in rating was found when comparing *R2*, *R3*, and *R4*. Remarkably, different trends can be observed for codec *C2*, for which only bitrates *R3 - R4* are to be considered statistically equivalent ($p = 0.055$), whereas all other touples for content *Longdress* present significant differences (*R1 - R2*: $p = 0.005$; *R1 - R3*: $p <$ .001; *R1 - R4*: $p <$ .001; *R2 - R3*: $p <$ .001; *R2 - R4*: $p <$ .001). For content *Loot*, statistical differences are observed, for codec *C1*, among all bitrates, bar *R2 - R3* ($p = 0.142$) and *R3 - R4* ($p = 1$); the rest falls below the significance level (*R1 - R2*: $p <$ .001; *R1 - R3*: $p <$ .001; *R1 - R4*: $p <$ .001; *R2 - R4*: $p = 0.004$). For codec *C2*, however, a different trend is observed: bitrates *R1 - R2* are the only touple, for *Loot*, for which no statistical difference is found ($p = 0.377$), whereas all other cases present statistically significant differences ($p <$ .001 for all touples). Content *Red and black* exhibits similar behaviour as *Longdress*: for codec *C1*, only differences among bitrate *R1* with all the other bitrates are significant (*R1 - R2*: $p <$ .001; *R1 - R3*: $p <$ .001; *R1 - R4*: $p <$ .001), whereas for codec *C2*, all bitrate touples are statistically different at 5% significance level (*R1 - R2*: $p = 0.018$; *R1 - R3*: $p <$ .001; *R1 - R4*: $p <$ .001; *R2 - R3*: $p <$ .001; *R2 - R4*: $p <$ .001; *R3 - R4*: $p <$ .001). For content *Soldier*, significant differences were found, for codec *C1*, for all bitrate touples, bar *R3 - R4* ($p = 0.648$; for all other touples, $p <$ .001); conversely, for codec *C2*, the only bitrates who did not exhibit significant differences were *R1 - R2* ($p = 0.373$; for all other touples, $p <$ .001). This seems to indicate that generally, for codec *C1* statistical differences in score distributions are usually found between lower bitrates, whereas the highest bitrates have a more uniform behaviour; however, for codec *C2*, more differences can be found across score distribution for all the bitrates, bar certain cases (such
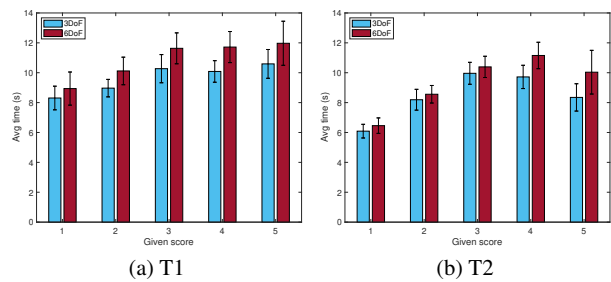
Fig. 5: Average time spent looking at the sequence (in seconds) and relative CIs, against score given to the sequence, for 3DoF (blue) and 6DoF (red), in test T1 (left) and T2 (right).

as *Loot* and *Soldier*) for which the lowest bitrates are deemed equivalent. Several other combinations of the three factors under exam were deemed statistically significant, more than what we could cover in this pages: we refer interested readers to the appendix for a full coverage of the post-hoc interaction results.

4.3 Additional questionnaires and interaction data

4.3.1 IPQ & SSQ Questionnaires

For T1 and T2, the collected IPQ data under each subscale are all normally distributed as examined by the Shapiro-Wilk test ($p > 0.05$). A paired sample t-test was applied to check the differences between 3DoF and 6DoF in terms of SP, INV, REAL and G. For T1, there was a significant difference in SP between 3DoF (M=4.13, SD=0.92) and 6DoF (M=5.04, SD=0.67), t(26)=-4.44, $p <$ .001, Cohen's d = 0.52 and also a significant difference in G between 3DoF (M=4.11, SD=1.28) and 6DoF (M=4.96, SD=1.13), t(26)=-2.60, $p <$ .01, Cohen's d = 0.64. For T2, SP was also significantly different in 3DoF (M=4.16, SD=1.17) and 6DoF (M=4.83, SD=1.12), t(24)=-3.48, $p <$ .01, Cohen's d = 0.45 and so was G between 3DoF (M=4.20, SD=1.61) and 6DoF (M=5.08, SD=1.19), t(24)=-3.56, $p <$ .01, Cohen's d = 0.71. Other factors showed no significant differences between 3DoF and 6DoF in both T1 and T2.

With respect to SSQ, no significant differences ($p > 0.05$) were found between 3DoF and 6DoF in terms of cybersickness. We further tested whether there were order effects in experiencing cybersickness, where half of the participants started with 6DoF as the first condition and 3DoF as the second, and the remainder the inverse. No significant differences ($p > 0.05$) were found for any order effects in experiencing cybersickness.

4.3.2 Interaction time

Interaction time was found to be strongly correlated with MOS values in a study conducted on light field image quality assessment [49], as well as in studies conducted with point cloud contents in interactive environments [9]. In particular, it was found that users tended to spend more time interacting with contents at high quality, whereas for low quality scores, less time was spent looking at the contents. In order to see whether similar trends could be observed in our data, we compared the average time spent watching the sequence in 3DoF and 6DoF, separately for each quality score given by the participants. Since no interactivity was present in the 2DTV condition, the data was discarded for the analysis. Results are shown in Fig. 5. A positive trend can be observed between the given score and the average time spent looking at the sequence, with the exception of score 5, which for test T2 shows a negative trend with respect to the time. However, it should be considered that on average, a small percentage of scores equal to 5 were given in test T2 (10% of the total scores), thus, variations may be due to the difference in sample size. It is also worth noting that, on average, participants spent more time looking at the sequences in 6DoF, with respect to the 3DoF case. Indeed, several participants pointed out that the lowest scores were the fastest to be given, whereas for higher quality, it was harder to decide on the rating.

4.3.3 Interviews

The interviews were only conducted for the VR conditions, due to time limitations. We asked the same interview questions for T1 and T2; so, we combined the interview transcripts of 52 participants (T1=27, T2=25). Participants were labelled as T1P1-T1P27 or T2P1-T2P25. The categorized answers are presented as follows:

Factors considered when assessing quality. 57% of the participants mentioned that they assessed the quality based on three criteria: 1) overall outline and pattern distortion on body and on clothes, 2) natural gestures and movements of the digital humans, and 3) visual artifacts such as blockiness, blurriness, and extraneous floating artifacts. As T2P3 commented, *"I paid attention to the blurriness of the clothing patterns, the fingers, and whether the gestures or movements were smooth. "* 48% of the participants mentioned the quality assessment criteria are content related, who agreed that it is easier to spot artifacts for the content with complex patterns (e.g., *Long dress*) and dominant colors (e.g., *Red and black*) than the content with uniformed colors (e.g., *Soldier* and *Sarge*). T2P5 said, *"The two ladies were easier [to assess the visual quality], because their clothes have strong colors. The man playing keyboard or something is quite difficult. His clothes were mainly monotone."* 46% of the participants

considered facial expressions as an unignorable factor for quality assessment, which they believe is an important cue for social connectedness. For example, T1P15 mentioned, *"The robotic lady was static and had no [facial] expression at all. It was difficult to tell the difference [between different quality levels]. "* Similarly, T2P8 said, *"If I could see her [the lady with red dress] smile and her teeth, I gave the score of fair to good. "* For the extraneous floating artifacts (e.g., bubbles flickering outside the digital humans), 23% found it very annoying and lowered the overall quality for the content, but a few participants (8%) thought these artifacts do not influence their quality judgement. T1P4 commented, *"The flickering blocks were annoying and distracting at the beginning, but later I got used to them. It felt like watching an old movie."*

Difficulties in assessment. 42% of the participants pointed out the difficulties in assessing the quality, especially for the high quality contents, which are not perfect and still have missing details like blurry faces or wrong fingers. 15% of the participants specifically pointed out that it is difficult to distinguish between quality level 3 to 5. As T2P21 mentioned, *"It was difficult to give [score] 5, the best ones were still missing many details like fingers or feet. I was hesitating all the time between [score] 4 and 5."* 17% of the participants commented that it gradually became easier in rating the quality when they adapted to the contents. So, the second viewing condition was easier for them. For example, T1P12 said, *"I noticed that the rating got easier as I got familiar to the quality levels, and had seen the best and the worst qualities."*

Comparison between 3DoF and 6DoF. 52% of the participants preferred 6DoF, because it allowed them to move closer to examine the details (e.g., shoes and fingers). They felt more realistic when walking in the virtual space. However, they also commented that 3DoF offered a fixed distance between them and digital humans, enabling a more stable and focused assessment. For example, T2P13 commented, *"Walking around [6DoF] allowed me to get really close [to the digital humans] and see more details, like pixel sizes, shoes, fingers. It felt more realistic. Sitting down [3DoF] has a distance [between me and the digital humans]. Sometimes, I found it difficult to assess the quality."* 21% of the participants preferred relaxation and passiveness in 3DoF, because they did not find much differences between 3DoF and 6DoF in terms of quality assessment, but they found 3DoF is less nauseous than 6DoF. As T1P13 mentioned, *"I felt more focused, secured and relaxed when sitting down. I got worried to be trapped by the cables. I also felt more dizzy when I walked around [in VR]."*

5 Discussion

5.1 Testing in VR

Results of our experiment indicate a very small, if not negligible, effect of viewing condition on the distribution of the scores. In particular, the viewing condition was deemed to have a significant effect on the distribution of the scores for the first set of contents we tested, revealing significant differences between VR testing and the 2DTV counterpart, with small effect sizes; for the second set of contents, no significant difference was spotted. The implications of it are twofold. On one hand, results show that the score distributions follow similar trends in VR with respect to passive video consumption, thus confirming the validity of testing volumetric contents on traditional 2D screens, as it has been done for the majority of tests performed in the literature. More specifically, no significant interaction was found, for both tests, between viewing condition and codec under exam, indicating that differences among compression solutions are not affected by the choice of displaying device and interaction paradigm. However, the interaction between viewing condition and contents was found to be significant for test T1: in particular, results indicate that differences among contents vary depending on the visualization medium. This might be due to a variety of factors: the possibility of interacting with the content, moving closer to inspect details; the presence of a fixed viewing point, which allows for easier comparison; the absence of confounding factors such as simulator-induced sickness or novelty effect. Particular care should be adopted in choosing contents depending on the type of test that needs to be carried, making sure that artifacts are visible at the distance that is selected for passive viewing, for example.

The second implication involves the constituents of quality of experience. The MOS of visual quality is only one of the factors that influences the quality of experience of a given user; other factors, such as presence and immersion, are equally important in determining the enjoyment of a given user using the system. Even though small or no effect of viewing condition on the MOS distribution was found, results of the IPQ revealed a strong effect of viewing condition on spatial presence and general sense of being there. Such factors should be taken into consideration when designing new experiments: if visual quality is the main constituent that needs to be assessed, traditional screens might be substituted (with caution) for VR assessment; however, if other factors need to be evaluated, such choice might have a larger impact.

5.2 Datasets

Despite the rich literature in point cloud acquisition and compression, few point cloud datasets are publicly available. This is especially true when considering point cloud datasets depicting photo-realistic humans. One of the most popular and widely used full-body dataset, created by 8i Labs [12], consists of only 4 individual contents, whereas the HHI Fraunhofer dataset has 1 individual content [13]. In the context of point cloud compression, such scarcity of available data may lead to compression solutions being designed, optimized and tested while considering a considerably narrow range of input data, thus leading to algorithms that are overfitted to the specifics of the acquisition method used to obtain the contents. The consequences of such a scenario are reflected in our results. Whereas for the contents assessed in test T2 a large difference was observed between codec V-PCC and the MPEG anchor, for the contents in test T1 the gap was markedly lower, and indeed the significance of the effect of the codec selection had a smaller effect size for test T1 with respect to test T2, as seen in section 4.1. Test T2 consisted of contents that had been used in multiple quality assessment experiments [7,8,37,44,47], notably including the performance evaluation of the upcoming MPEG standard [43]. On the other hand, test T1 included contents that have not been used so far in assessment of point cloud compression solutions. The discrepancies in the results of the subjective quality assessment campaign indicate that performance gains may vary considerably when new contents are evaluated. A larger body of contents depicting digital humans, involving several acquisition technologies, is needed in order to properly design, train and evaluate new compression solutions in a robust way.

5.3 Personal preferences and bias

Subjective evaluation experiments are complicated by many aspects of human psychology and viewing conditions, such as participants' vision ability, translation of quality perception into ranking scores, adaptations and personal preferences for contents. Through carefully following the ITU-T Recommendations P.913 [25], we are able to control some of the aspects. For example, eliminate the scores given by the participants with vision problems; train participants to help them understand the quality levels; randomize the stimuli and viewing conditions to minimize the order effects. However, we noticed that personal preferences towards certain contents are difficult to control. Satgunam et al. [41]) found that their participants were divided into two preference groups: prefer sharper content versus smoother content. Similarly, Kortum and Sullivan [30] found that the "desirability" of participants had an impact on video quality responses, with a more desirable video clip being given a higher rating. In our experiments, content *Queen* is generally given lower ratings with respect to the other contents. In the interviews, 40% of the participants showed their preference towards *Soldier*, due to his high-resolution facial features, unitoned clothes

and natural movements, whereas 27% expressed dislike towards *Queen*, because of her lifeless look and static gestures. Body motion has been shown to be important in increasing the naturalness of virtual characters, especially when involving complex motions [35]. Moreover, several studies have highlighted the importance of matching the appearance of the avatar to the naturalness of the motion, indicating that "appropriateness" between visual presentation and gesture plays an important role in realism [16, 31]. Our findings suggests that realism and naturalness of interaction might have an impact on the perceived visual quality of the contents as well. Quality assessment may need to be adjusted based on content and viewer preferences, and offering training with different contents, as well as account for factors such as realism, naturalness of motion, and uncanny valley effect.

5.4 Technological constraints and limitations

The two codecs used in this experiment introduce different distortions during compression. As the MPEG anchor codec uses the octree data structure to represent geometry, the number of points in the decoded cloud varies exponentially based on the tree depth. Thus, at lower bitrates, the decoded point clouds are quite sparse, and when the point size is increased to make them appear watertight, they have a block-y appearance. However, the low delay encoding and decoding of this codec makes it suitable for real time applications such as social VR. On the other hand, the V-PCC codec leverages existing 2D video codecs to compress both geometry and color, which introduces noise in terms of extraneous objects, and general geometric artifacts such as misaligned seams (see Figure 1). However, the approach yields better results at low bitrates, as demonstrated in our results. The codec is optimized for human perception of 2D video, which might lead to undesired results when applied to 3D objects in VR. The mapping from 3D to 2D is critical to codec performance, which explains why the encoding phase has high complexity. Decoding has a lower delay, as it benefits from hardware acceleration of video decoders on GPUs, making this approach suitable for on-demand streaming.

One of the main shortcoming of both compression solutions lays in their inability to reach visually-lossless quality, as demonstrated by our results. Achieving a visually pleasant result is of paramount importance for the market adoption of the technology; indeed, poor visual quality might lead consumers to tune off from the experience altogether [1]. Visual perception should be taken into account when designing compression solutions, especially at high bitrates, to ensure that in absence of strict bandwidth constraints, excellent quality can be achieved.

5.5 Rendering environment considerations

Previous research on subjective assessment of dynamic point cloud contents has been primarily conducted in desktop setups [2, 52], whereas VR/AR technologies have been employed with static content [6, 8], or limited amount of dynamic contents [53]. However, placing dynamic contents to be rendered in a VR/AR environment in real time, in order for users to interact, adds several technological constraints. In previous research on subjective assessment of point cloud content such as the MPEG standardisation activity [2], participants were asked to view a video of the point cloud sequence rendered from a predefined camera path. The same approach was used by van der Hooft et al. to subjectively and objectively assess the quality of adaptive streaming for point cloud contents [20]; however, the influence of camera paths on objective quality assessment was shown to be significant in [46]. In order to allow users to interact with the content in a VR/AR environment, the dynamic point clouds need to be rendered in real time. This is, however, extremely resource intensive, and poses many technical constraints. For our test in particular, the point clouds needed to be stored as uncompressed files, to avoid confounding factors with the compression solutions under evaluation. The point cloud files were stored as binary PLY files to allow faster read from disk. Yet, real-time progressive loading of the sequences was not possible, as the loading operation was interfering with the rendering, thus leading to drops in the frame rate. Waiting for each sequence to be loaded, on the other hand, was unattainable, as the read time from disk would mean long waiting times between one sequence and another, thus adding to subjects' fatigue. To fix the issue, we decided to load all sequences in physical memory before the test. However, this impacted the amount of sequences that could be tested in one session, as well as the length of each. New systems for rendering point clouds in real time, while respecting the constraints introduced by quality assessment scenarios, should be developed in order to foster research in the field.

5.6 Protocols for subjective assessment in VR

Choosing the right methodology to follow in order to collect users' opinions is a delicate matter, as it can influence the statistical power of the collected score, and in some cases lead to difference in results. Single stimulus methodologies, in particular, lead to larger CIs with respect to double stimulus methodologies, and are more subject to be influenced by individual content preference [25]. An early study comparing single and double stimulus methodologies for the evaluation of colorless point cloud contents indicated that the latter was more consistent in recognizing the level of impairment, as relative differences facilitate the rating task [3]. However, the study pointed out that the single stimulus methodology shows

more discrimination power for compression-like artifacts, albeit at the cost of wider CIs.

Double stimulus methodologies, while commonly used in video quality assessment and widely adopted in 2D-based quality assessment of point cloud contents [7, 43, 44], are tricky to adopt in VR technology, due to the difficulties in displaying both contents simultaneously in a perceptually satisfying way [36], while ensuring a fair comparison between the contents under evaluation. When dealing with interactive methodologies, in particular, synchronous display of any modification in viewport is usually enforced, to ensure that the two contents are always visible at the same condition [7, 49]. This is clearly challenging to implement in a 6DoF scenario, in which users are free to change their position in the VR space at any given time. Positioning the two contents side by side in the same virtual space would mean that, at any given time, they are seen from two different angles; the same problem would arise when temporal sequencing is employed. A toggle-based method like the one proposed in [36] is not applicable to moving sequences, as different frames would be seen between stimuli.

In our study, we saw that content preference had an impact on the ratings, as several contents were deemed of lower quality, as the scores given to the HR exemplify. Such bias resulted in a reduced rating range for the contents. Results of the interviews also pointed out that naturalness of gestures were an important criteria in assessing the visual quality. Such components would not be normally evaluated in a double stimulus scenario; however, they are important in understanding how human perception reacts to digital humans.

6 Conclusion

In this paper, we extend our previous work by comparing the performance of the point cloud compression standard V-PCC against an octree-based anchor codec (MPEG anchor). Participants were invited to assess the quality of digital humans represented as dynamic point clouds, in 2DTV screen, as well as VR with 3DoF and 6DoF conditions. Results indicate a small effect of viewing condition on the final scores for one of the two sets of contents under test. Moreover, results show that codec V-PCC has a more favorable performance than the MPEG anchor, especially at low bit-rates. For the highest bit-rate, the two codecs are often statistically equivalent. The contents under test appear to have a significant influence on how the scores are distributed; thus, new data sets are needed in order to comprehensively evaluate compression distortions. Moreover, current encoding solutions, while efficient at low bitrates, are unable to provide visually lossless results, even when large volumes of data are available, revealing significant shortcomings in point cloud compression. We also point out that commonly-used double stimulus methodologies for quality evaluation often reduce the rating task to a difference

recognition, while insights on the quality of the original contents are missed. The raw data is made available at the following link: `https://github.com/cwi-dis/2DTV_VR_QoE`.

References

1. OTT: Beyond Entertainment Consumer Survey Report. `https://www.conviva.com/research/ott-beyond-entertainment/`

2. Call for proposals for point cloud compression iso/iec jtc1/sc29 wg11 n16732, geneva ch (2017)

3. Alexiou, E., Ebrahimi, T.: On the performance of metrics to predict quality in point cloud representations. In: Applications of Digital Image Processing XL, vol. 10396, p. 103961H. International Society for Optics and Photonics (2017)

4. Alexiou, E., Ebrahimi, T.: Impact of visualisation strategy for subjective quality assessment of point clouds. In: 2018 IEEE International Conference on Multimedia & Expo Workshops (ICMEW), pp. 1–6. IEEE (2018)

5. Alexiou, E., Tung, K., Ebrahimi, T.: Towards neural network approaches for point cloud compression. In: Applications of Digital Image Processing XLIII, vol. 11510, p. 1151008. International Society for Optics and Photonics (2020)

6. Alexiou, E., Upenik, E., Ebrahimi, T.: Towards subjective quality assessment of point cloud imaging in augmented reality. In: 2017 IEEE 19th International Workshop on Multimedia Signal Processing (MMSP), pp. 1–6. IEEE (2017)

7. Alexiou, E., Viola, I., Borges, T.M., Fonseca, T.A., de Queiroz, R.L., Ebrahimi, T.: A comprehensive study of the rate-distortion performance in mpeg point cloud compression. APSIPA Transactions on Signal and Information Processing **8**, 27 (2019). DOI 10.1017/ATSIP.2019.20. URL `http://infoscience.epfl.ch/record/272124`

8. Alexiou, E., Xu, P., Ebrahimi, T.: Towards modelling of visual saliency in point clouds for immersive applications. In: 26th IEEE International Conference on Image Processing (ICIP) (2019)

9. Alexiou, E., Yang, N., Ebrahimi, T.: Pointxr: A toolbox for visualization and subjective evaluation of point clouds in virtual reality. In: 2020 Twelfth International Conference on Quality of Multimedia Experience (QoMEX), pp. 1–6. IEEE (2020)

10. Cao, C., Preda, M., Zakharchenko, V., Jang, E.S., Zaharia, T.: Compression of sparse and dense dynamic point clouds–methods and standards. Proceedings of the IEEE (2021)

11. Cohen, R.A., Tian, D., Vetro, A.: Point cloud attribute compression using 3-d intra prediction and shape-adaptive transforms. In: 2016 Data Compression Conference (DCC), pp. 141–150. IEEE (2016)

12. d'Eon, E., Harrison, B., Myers, T., Chou, P.A.: 8i Voxelized Full Bodies - A Voxelized Point Cloud Dataset, ISO/IEC JTC1/SC29 Joint WG11/WG1 (MPEG/JPEG) input document WG11M40059/WG1M74006, Geneva (2017)

13. Ebner, T., Feldmann, I., Schreer, O., Kauff, P., v. Unger, T.: HHI Point cloud dataset of a boxing trainer, ISO/IEC JTC1/SC29 Joint WG11/WG1 (MPEG/JPEG) input document MPEG2018/m42921, Ljubljana (2018)

14. Ebrahimi, T., Foessel, S., Pereira, F., Schelkens, P.: Jpeg pleno: Toward an efficient representation of visual reality. Ieee Multimedia **23**(4), 14–20 (2016)

15. Elkin, L.A., Kay, M., Higgins, J.J., Wobbrock, J.O.: An aligned rank transform procedure for multifactor contrast tests. arXiv preprint arXiv:2102.11824 (2021)

16. Ferstl, Y., Thomas, S., Guard, C., Ennis, C., McDonnell, R.: Human or robot? investigating voice, appearance and gesture motion realism of conversational social agents. In: Proceedings of the 21st ACM International Conference on Intelligent Virtual Agents, pp. 76–83 (2021)

17. Guarda, A.F., Rodrigues, N.M., Pereira, F.: Deep learning-based point cloud coding: A behavior and performance study. In: 2019 8th European Workshop on Visual Information Processing (EUVIP), pp. 34–39. IEEE (2019)

18. Guarda, A.F., Rodrigues, N.M., Pereira, F.: Point cloud coding: Adopting a deep learning-based approach. In: 2019 Picture Coding Symposium (PCS), pp. 1–5. IEEE (2019)

19. Guarda, A.F., Rodrigues, N.M., Pereira, F.: Deep learning-based point cloud geometry coding: Rd control through implicit and explicit quantization. In: 2020 IEEE International Conference on Multimedia & Expo Workshops (ICMEW), pp. 1–6. IEEE (2020)

20. van der Hooft, J., Vega, M.T., Timmerer, C., Begen, A.C., De Turck, F., Schatz, R.: Objective and subjective qoe evaluation for adaptive point cloud streaming. In: 2020 twelfth international conference on quality of multimedia experience (QoMEX), pp. 1–6. IEEE (2020)

21. ISO/IEC DIS 23090-5: Geometry-based point cloud compression. International Organization for Standardization

22. ISO/IEC DIS 23090-5: Visual volumetric video-based coding (V3C) and video-based point cloud compression (V-PCC). International Organization for Standardization (2021)

23. ITU-R BT.500-13: Methodology for the subjective assessment of the quality of television pictures. International Telecommunication Union (2012)

24. ITU-T P.910: Subjective video quality assessment methods for multimedia applications. International Telecommunication Union (2008)

25. ITU-T P.913: Methods for the subjective assessment of video quality, audio quality and audiovisual quality of Internet video and distribution quality television in any environment. International Telecommunication Union (2016)

26. Jackins, C.L., Tanimoto, S.L.: Oct-trees and their use in representing three-dimensional objects. Computer Graphics and Image Processing 14(3), 249–270 (1980)

27. Jang, E.S., Preda, M., Mammou, K., Tourapis, A.M., Kim, J., Graziosi, D.B., Rhyu, S., Budagavi, M.: Video-based point-cloud-compression standard in mpeg: from evidence collection to committee draft [standards in a nutshell]. IEEE Signal Processing Magazine 36(3), 118–123 (2019)

28. Kay, M., Wobbrock, J.: mjskay/artool: Artool 0.10.6 (2019). DOI 10.5281/zenodo.2556415. URL https://doi.org/10.5281/zenodo.2556415

29. Kennedy, R.S., Lane, N.E., Berbaum, K.S., Lilienthal, M.G.: Simulator sickness questionnaire: An enhanced method for quantifying simulator sickness. The international journal of aviation psychology 3(3), 203–220 (1993)

30. Kortum, P., Sullivan, M.: The effect of content desirability on subjective video quality ratings. Human factors 52(1), 105–118 (2010)

31. Kucherenko, T., Jonell, P., Yoon, Y., Wolfert, P., Henter, G.E.: A large, crowdsourced evaluation of gesture generation systems on common data: The genea challenge 2020. In: 26th International Conference on Intelligent User Interfaces, pp. 11–21 (2021)

32. Mammou, K.: PCC test model category 2 v0. ISO/IEC JTC1/SC29/WG11 N17248 1 (2017)

33. Meagher, D.: Geometric modeling using octree encoding. Computer graphics and image processing 19(2), 129–147 (1982)

34. Mekuria, R., Blom, K., Cesar, P.: Design, implementation, and evaluation of a point cloud codec for tele-immersive video. IEEE Transactions on Circuits and Systems for Video Technology 27(4), 828–842 (2017)

35. Neff, M.: Hand gesture synthesis for conversational characters. Handbook of Human Motion pp. 1–12 (2016)

36. Perrin, A.F., Bist, C., Cozot, R., Ebrahimi, T.: Measuring quality of omnidirectional high dynamic range content. In: Applications of Digital Image Processing XL, vol. 10396, p. 1039613. International Society for Optics and Photonics (2017)

37. Perry, S., Cong, H.P., da Silva Cruz, L.A., Prazeres, J., Pereira, M., Pinheiro, A., Dumic, E., Alexiou, E., Ebrahimi, T.: Quality evaluation of static point clouds encoded using mpeg codecs. In: 2020 IEEE International Conference on Image Processing (ICIP), pp. 3428–3432. IEEE (2020)

38. Quach, M., Valenzise, G., Dufaux, F.: Learning convolutional transforms for lossy point cloud geometry compression. In: 2019 IEEE International Conference on Image Processing (ICIP), pp. 4320–4324. IEEE (2019)

39. Quach, M., Valenzise, G., Dufaux, F.: Improved deep point cloud geometry compression. In: 2020 IEEE 22nd International Workshop on Multimedia Signal Processing (MMSP), pp. 1–6. IEEE (2020)

40. Queiroz, R.D., Chou, P.A.: Compression of 3D Point Clouds Using a Region-Adaptive Hierarchical Transform. IEEE Transactions on Image Processing 25 (2016)

41. Satgunam, P.N., Woods, R.L., Bronstad, P.M., Peli, E.: Factors affecting enhanced video quality preferences. IEEE Transactions on Image Processing 22(12), 5146–5157 (2013)

42. Schubert, T.W.: The sense of presence in virtual environments: A three-component scale measuring spatial presence, involvement, and realness. Zeitschrift für Medienpsychologie 15(2), 69–71 (2003)

43. Schwarz, S., Preda, M., Baroncini, V., Budagavi, M., Cesar, P., Chou, P.A., Cohen, R.A., Krivokuća, M., Lasserre, S., Li, Z., et al.: Emerging MPEG standards for point cloud compression. IEEE Journal on Emerging and Selected Topics in Circuits and Systems 9(1), 133–148 (2018)

44. da Silva Cruz, L.A., Dumić, E., Alexiou, E., Prazeres, J., Duarte, R., Pereira, M., Pinheiro, A., Ebrahimi, T.: Point cloud quality evaluation: Towards a definition for test conditions. In: 2019 Eleventh International Conference on Quality of Multimedia Experience (QoMEX), pp. 1–6. IEEE (2019)

45. Subramanyam, S., Li, J., Viola, I., Cesar, P.: Comparing the quality of highly realistic digital humans in 3dof and 6dof: A volumetric video case study. In: 2020 IEEE Conference on Virtual Reality and 3D User Interfaces (VR), pp. 127–136. IEEE (2020)

46. Subramanyam, S., Viola, I., Hanjalic, A., Cesar, P.: User centered adaptive streaming of dynamic point clouds with low complexity tiling. In: Proceedings of the 28th ACM International Conference on Multimedia, pp. 3669–3677 (2020)

47. Torlig, E.M., Alexiou, E., Fonseca, T.A., de Queiroz, R.L., Ebrahimi, T.: A novel methodology for quality assessment of voxelized point clouds. In: Applications of Digital Image Processing XLI, vol. 10752, p. 107520I. International Society for Optics and Photonics (2018)

48. TT Tran, H., Ngoc, N.P., Pham, C.T., Jung, Y.J., Thang, T.C.: A subjective study on user perception aspects in virtual reality. Applied Sciences 9(16), 3384 (2019)

49. Viola, I., Ebrahimi, T.: A new framework for interactive quality assessment with application to light field coding. In: Applications of Digital Image Processing XL, vol. 10396, p. 103961F. International Society for Optics and Photonics (2017)

50. Wang, J., Zhu, H., Liu, H., Ma, Z.: Lossy point cloud geometry compression via end-to-end learning. IEEE Transactions on Circuits and Systems for Video Technology (2021)

51. Wobbrock, J.O., Findlater, L., Gergle, D., Higgins, J.J.: The Aligned Rank Transform for nonparametric factorial analyses using only ANOVA procedures. In: Proceedings of the SIGCHI conference on human factors in computing systems, pp. 143–146. ACM (2011)

52. Zerman, E., Gao, P., Ozcinar, C., Smolic, A.: Subjective and objective quality assessment for volumetric video compression. In: Fast track article for IST International Symposium on Electronic Imaging 2019: Image Quality and System Performance XVI proceedings (2019)

53. Zerman, E., Kulkarni, R., Smolic, A.: User behaviour analysis of volumetric video in augmented reality. In: 2021 13th International Conference on Quality of Multimedia Experience (QoMEX), pp. 129–132. IEEE (2021)

54. Zerman, E., Ozcinar, C., Gao, P., Smolic, A.: Textured mesh vs coloured point cloud: A subjective study for volumetric video compression. In: 2020 Twelfth International Conference on Quality of Multimedia Experience (QoMEX), pp. 1–6. IEEE (2020)

55. Zhang, C., Florencio, D., Loop, C.: Point cloud attribute compression with graph transform. Image Processing (ICIP), 2014 IEEE International Conference on (2014)

56. Zhang, J., Huang, W., Zhu, X., Hwang, J.N.: A subjective quality evaluation for 3D point cloud models. In: 2014 International Conference on Audio, Language and Image Processing, pp. 827–831. IEEE (2014)

Appendix A

Table 5: Contrast test between factors DoF and Content

contrast	estimate	SE	df	t.ratio	p.value
3DoF, Manfred - 3DoF, Sarge	-9.0337	60.7066	2294.00	-0.149	1.0000
3DoF, Manfred - 3DoF, Despoina	178.6466	60.7066	2294.00	2.943	0.1268
3DoF, Manfred - 3DoF, Queen	-388.5697	60.7066	2294.00	-6.401	<.0001
3DoF, Manfred - 6DoF, Manfred	-88.2236	108.4749	126.03	-0.813	0.9996
3DoF, Manfred - 6DoF, Sarge	-72.3942	108.4749	126.03	-0.667	0.9999
3DoF, Manfred - 6DoF, Despoina	279.4808	108.4749	126.03	2.576	0.3044
3DoF, Manfred - 6DoF, Queen	-188.9303	108.4749	126.03	-1.742	0.8452
3DoF, Manfred - 2DTV, Manfred	-30.8302	109.5543	126.03	-0.281	1.0000
3DoF, Manfred - 2DTV, Sarge	189.7498	109.5543	126.03	1.732	0.8499
3DoF, Manfred - 2DTV, Despoina	-84.0802	109.5543	126.03	-0.767	0.9998
3DoF, Manfred - 2DTV, Queen	-300.8752	109.5543	126.03	-2.746	0.2166
3DoF, Sarge - 3DoF, Despoina	187.6803	60.7066	2294.00	3.092	0.0848
3DoF, Sarge - 3DoF, Queen	-379.5361	60.7066	2294.00	-6.252	<.0001
3DoF, Sarge - 6DoF, Manfred	-79.1899	108.4749	126.03	-0.730	0.9999
3DoF, Sarge - 6DoF, Sarge	-63.3606	108.4749	126.03	-0.584	1.0000
3DoF, Sarge - 6DoF, Despoina	288.5144	108.4749	126.03	2.660	0.2590
3DoF, Sarge - 6DoF, Queen	-179.8966	108.4749	126.03	-1.658	0.8831
3DoF, Sarge - 2DTV, Manfred	-21.7965	109.5543	126.03	-0.199	1.0000
3DoF, Sarge - 2DTV, Sarge	198.7835	109.5543	126.03	1.814	0.8071
3DoF, Sarge - 2DTV, Despoina	-75.0465	109.5543	126.03	-0.685	0.9999
3DoF, Sarge - 2DTV, Queen	-291.8415	109.5543	126.03	-2.664	0.2568
3DoF, Despoina - 3DoF, Queen	-567.2163	60.7066	2294.00	-9.344	<.0001
3DoF, Despoina - 6DoF, Manfred	-266.8702	108.4749	126.03	-2.460	0.3747
3DoF, Despoina - 6DoF, Sarge	-251.0409	108.4749	126.03	-2.314	0.4722
3DoF, Despoina - 6DoF, Despoina	100.8341	108.4749	126.03	0.930	0.9987
3DoF, Despoina - 6DoF, Queen	-367.5769	108.4749	126.03	-3.389	0.0422
3DoF, Despoina - 2DTV, Manfred	-209.4768	109.5543	126.03	-1.912	0.7495
3DoF, Despoina - 2DTV, Sarge	11.1032	109.5543	126.03	0.101	1.0000
3DoF, Despoina - 2DTV, Despoina	-262.7268	109.5543	126.03	-2.398	0.4151
3DoF, Despoina - 2DTV, Queen	-479.5218	109.5543	126.03	-4.377	0.0015
3DoF, Queen - 6DoF, Manfred	300.3462	108.4749	126.03	2.769	0.2064
3DoF, Queen - 6DoF, Sarge	316.1755	108.4749	126.03	2.915	0.1485
3DoF, Queen - 6DoF, Despoina	668.0505	108.4749	126.03	6.159	<.0001
3DoF, Queen - 6DoF, Queen	199.6394	108.4749	126.03	1.840	0.7924
3DoF, Queen - 2DTV, Manfred	357.7395	109.5543	126.03	3.265	0.0601
3DoF, Queen - 2DTV, Sarge	578.3195	109.5543	126.03	5.279	<.0001
3DoF, Queen - 2DTV, Despoina	304.4895	109.5543	126.03	2.779	0.2018
3DoF, Queen - 2DTV, Queen	87.6945	109.5543	126.03	0.800	0.9997
6DoF, Manfred - 6DoF, Sarge	15.8293	60.7066	2294.00	0.261	1.0000
6DoF, Manfred - 6DoF, Despoina	367.7043	60.7066	2294.00	6.057	<.0001
6DoF, Manfred - 6DoF, Queen	-100.7067	60.7066	2294.00	-1.659	0.8865
6DoF, Manfred - 2DTV, Manfred	57.3934	109.5543	126.03	0.524	1.0000
6DoF, Manfred - 2DTV, Sarge	277.9734	109.5543	126.03	2.537	0.3272
6DoF, Manfred - 2DTV, Despoina	4.1434	109.5543	126.03	0.038	1.0000
6DoF, Manfred - 2DTV, Queen	-212.6516	109.5543	126.03	-1.941	0.7312
6DoF, Sarge - 6DoF, Despoina	351.8750	60.7066	2294.00	5.796	<.0001
6DoF, Sarge - 6DoF, Queen	-116.5361	60.7066	2294.00	-1.920	0.7470
6DoF, Sarge - 2DTV, Manfred	41.5640	109.5543	126.03	0.379	1.0000

Table 5 – *Continued from previous page*

contrast	estimate	SE	df	t.ratio	p.value
6DoF, Sarge - 2DTV, Sarge	262.1440	109.5543	126.03	2.393	0.4187
6DoF, Sarge - 2DTV, Despoina	-11.6860	109.5543	126.03	-0.107	1.0000
6DoF, Sarge - 2DTV, Queen	-228.4810	109.5543	126.03	-2.086	0.6338
6DoF, Despoina - 6DoF, Queen	-468.4111	60.7066	2294.00	-7.716	<.0001
6DoF, Despoina - 2DTV, Manfred	-310.3110	109.5543	126.03	-2.832	0.1794
6DoF, Despoina - 2DTV, Sarge	-89.7310	109.5543	126.03	-0.819	0.9996
6DoF, Despoina - 2DTV, Despoina	-363.5610	109.5543	126.03	-3.319	0.0517
6DoF, Despoina - 2DTV, Queen	-580.3560	109.5543	126.03	-5.297	<.0001
6DoF, Queen - 2DTV, Manfred	158.1001	109.5543	126.03	1.443	0.9524
6DoF, Queen - 2DTV, Sarge	378.6801	109.5543	126.03	3.457	0.0345
6DoF, Queen - 2DTV, Despoina	104.8501	109.5543	126.03	0.957	0.9983
6DoF, Queen - 2DTV, Queen	-111.9449	109.5543	126.03	-1.022	0.9969
2DTV, Manfred - 2DTV, Sarge	220.5800	61.9088	2294.00	3.563	0.0193
2DTV, Manfred - 2DTV, Despoina	-53.2500	61.9088	2294.00	-0.860	0.9994
2DTV, Manfred - 2DTV, Queen	-270.0450	61.9088	2294.00	-4.362	0.0008
2DTV, Sarge - 2DTV, Despoina	-273.8300	61.9088	2294.00	-4.423	0.0006
2DTV, Sarge - 2DTV, Queen	-490.6250	61.9088	2294.00	-7.925	<.0001
2DTV, Despoina - 2DTV, Queen	-216.7950	61.9088	2294.00	-3.502	0.0238

Results are averaged over the levels of: Codecs, Bitrates

Degrees-of-freedom method: kenward-roger

P value adjustment: tukey method for comparing a family of 12 estimates

Table 6: Contrast test between factors DoF and Content

contrast	estimate	SE	df	t.ratio	p.value
Manfred, C1 - Manfred, C2	259.8001	49.6388	2294	5.234	<.0001
Manfred, C1 - Sarge, C1	37.6988	49.6388	2294	0.759	0.9950
Manfred, C1 - Sarge, C2	358.0433	49.6388	2294	7.213	<.0001
Manfred, C1 - Despoina, C1	181.0136	49.6388	2294	3.647	0.0066
Manfred, C1 - Despoina, C2	435.7672	49.6388	2294	8.779	<.0001
Manfred, C1 - Queen, C1	-103.4447	49.6388	2294	-2.084	0.4256
Manfred, C1 - Queen, C2	-141.3435	49.6388	2294	-2.847	0.0842
Manfred, C2 - Sarge, C1	-222.1013	49.6388	2294	-4.474	0.0002
Manfred, C2 - Sarge, C2	98.2432	49.6388	2294	1.979	0.4963
Manfred, C2 - Despoina, C1	-78.7865	49.6388	2294	-1.587	0.7582
Manfred, C2 - Despoina, C2	175.9671	49.6388	2294	3.545	0.0095
Manfred, C2 - Queen, C1	-363.2449	49.6388	2294	-7.318	<.0001
Manfred, C2 - Queen, C2	-401.1436	49.6388	2294	-8.081	<.0001
Sarge, C1 - Sarge, C2	320.3445	49.6388	2294	6.454	<.0001
Sarge, C1 - Despoina, C1	143.3147	49.6388	2294	2.887	0.0756
Sarge, C1 - Despoina, C2	398.0683	49.6388	2294	8.019	<.0001
Sarge, C1 - Queen, C1	-141.1436	49.6388	2294	-2.843	0.0851
Sarge, C1 - Queen, C2	-179.0423	49.6388	2294	-3.607	0.0076
Sarge, C2 - Despoina, C1	-177.0297	49.6388	2294	-3.566	0.0088
Sarge, C2 - Despoina, C2	77.7238	49.6388	2294	1.566	0.7708
Sarge, C2 - Queen, C1	-461.4881	49.6388	2294	-9.297	<.0001
Sarge, C2 - Queen, C2	-499.3868	49.6388	2294	-10.060	<.0001
Despoina, C1 - Despoina, C2	254.7536	49.6388	2294	5.132	<.0001
Despoina, C1 - Queen, C1	-284.4583	49.6388	2294	-5.731	<.0001
Despoina, C1 - Queen, C2	-322.3571	49.6388	2294	-6.494	<.0001
Despoina, C2 - Queen, C1	-539.2119	49.6388	2294	-10.863	<.0001

Table 6 – *Continued from previous page*

contrast	estimate	SE	df	t.ratio	p.value
Despoina, C2 - Queen, C2	-577.1106	49.6388	2294	-11.626	<.0001
Queen, C1 - Queen, C2	-37.8987	49.6388	2294	-0.763	0.9949

Results are averaged over the levels of: DoF, Bitrates

Degrees-of-freedom method: kenward-roger

P value adjustment: tukey method for comparing a family of 8 estimates

Table 7: Contrast test between factors Content and Bitrate

contrast	estimate	SE	df	t.ratio	p.value
Manfred, R1 - Manfred, R2	-261.0203	56.8360	2294	-4.593	0.0005
Manfred, R1 - Manfred, R3	-813.6400	56.8360	2294	-14.316	<.0001
Manfred, R1 - Manfred, R4	-1080.8721	56.8360	2294	-19.017	<.0001
Manfred, R1 - Sarge, R1	90.9803	56.8360	2294	1.601	0.9684
Manfred, R1 - Sarge, R2	-221.5797	56.8360	2294	-3.899	0.0097
Manfred, R1 - Sarge, R3	-794.1628	56.8360	2294	-13.973	<.0001
Manfred, R1 - Sarge, R4	-996.3062	56.8360	2294	-17.529	<.0001
Manfred, R1 - Despoina, R1	156.6036	56.8360	2294	2.755	0.2961
Manfred, R1 - Despoina, R2	-85.3759	56.8360	2294	-1.502	0.9824
Manfred, R1 - Despoina, R3	-649.9931	56.8360	2294	-11.436	<.0001
Manfred, R1 - Despoina, R4	-1005.8467	56.8360	2294	-17.697	<.0001
Manfred, R1 - Queen, R1	-111.2328	56.8360	2294	-1.957	0.8485
Manfred, R1 - Queen, R2	-697.9362	56.8360	2294	-12.280	<.0001
Manfred, R1 - Queen, R3	-1025.7954	56.8360	2294	-18.048	<.0001
Manfred, R1 - Queen, R4	-1068.4754	56.8360	2294	-18.799	<.0001
Manfred, R2 - Manfred, R3	-552.6197	56.8360	2294	-9.723	<.0001
Manfred, R2 - Manfred, R4	-819.8518	56.8360	2294	-14.425	<.0001
Manfred, R2 - Sarge, R1	352.0005	56.8360	2294	6.193	<.0001
Manfred, R2 - Sarge, R2	39.4405	56.8360	2294	0.694	1.0000
Manfred, R2 - Sarge, R3	-533.1426	56.8360	2294	-9.380	<.0001
Manfred, R2 - Sarge, R4	-735.2859	56.8360	2294	-12.937	<.0001
Manfred, R2 - Despoina, R1	417.6238	56.8360	2294	7.348	<.0001
Manfred, R2 - Despoina, R2	175.6444	56.8360	2294	3.090	0.1344
Manfred, R2 - Despoina, R3	-388.9728	56.8360	2294	-6.844	<.0001
Manfred, R2 - Despoina, R4	-744.8264	56.8360	2294	-13.105	<.0001
Manfred, R2 - Queen, R1	149.7874	56.8360	2294	2.635	0.3741
Manfred, R2 - Queen, R2	-436.9159	56.8360	2294	-7.687	<.0001
Manfred, R2 - Queen, R3	-764.7751	56.8360	2294	-13.456	<.0001
Manfred, R2 - Queen, R4	-807.4551	56.8360	2294	-14.207	<.0001
Manfred, R3 - Manfred, R4	-267.2321	56.8360	2294	-4.702	0.0003
Manfred, R3 - Sarge, R1	904.6203	56.8360	2294	15.916	<.0001
Manfred, R3 - Sarge, R2	592.0603	56.8360	2294	10.417	<.0001
Manfred, R3 - Sarge, R3	19.4772	56.8360	2294	0.343	1.0000
Manfred, R3 - Sarge, R4	-182.6662	56.8360	2294	-3.214	0.0958
Manfred, R3 - Despoina, R1	970.2436	56.8360	2294	17.071	<.0001
Manfred, R3 - Despoina, R2	728.2641	56.8360	2294	12.813	<.0001
Manfred, R3 - Despoina, R3	163.6469	56.8360	2294	2.879	0.2262
Manfred, R3 - Despoina, R4	-192.2067	56.8360	2294	-3.382	0.0581
Manfred, R3 - Queen, R1	702.4072	56.8360	2294	12.358	<.0001
Manfred, R3 - Queen, R2	115.7038	56.8360	2294	2.036	0.8050
Manfred, R3 - Queen, R3	-212.1554	56.8360	2294	-3.733	0.0179
Manfred, R3 - Queen, R4	-254.8354	56.8360	2294	-4.484	0.0008

Table 7 – *Continued from previous page*

contrast	estimate	SE	df	t.ratio	p.value
Manfred, R4 - Sarge, R1	1171.8523	56.8360	2294	20.618	<.0001
Manfred, R4 - Sarge, R2	859.2923	56.8360	2294	15.119	<.0001
Manfred, R4 - Sarge, R3	286.7092	56.8360	2294	5.044	0.0001
Manfred, R4 - Sarge, R4	84.5659	56.8360	2294	1.488	0.9839
Manfred, R4 - Despoina, R1	1237.4756	56.8360	2294	21.773	<.0001
Manfred, R4 - Despoina, R2	995.4962	56.8360	2294	17.515	<.0001
Manfred, R4 - Despoina, R3	430.8790	56.8360	2294	7.581	<.0001
Manfred, R4 - Despoina, R4	75.0254	56.8360	2294	1.320	0.9952
Manfred, R4 - Queen, R1	969.6392	56.8360	2294	17.060	<.0001
Manfred, R4 - Queen, R2	382.9359	56.8360	2294	6.738	<.0001
Manfred, R4 - Queen, R3	55.0767	56.8360	2294	0.969	0.9999
Manfred, R4 - Queen, R4	12.3967	56.8360	2294	0.218	1.0000
Sarge, R1 - Sarge, R2	-312.5600	56.8360	2294	-5.499	<.0001
Sarge, R1 - Sarge, R3	-885.1431	56.8360	2294	-15.574	<.0001
Sarge, R1 - Sarge, R4	-1087.2864	56.8360	2294	-19.130	<.0001
Sarge, R1 - Despoina, R1	65.6233	56.8360	2294	1.155	0.9989
Sarge, R1 - Despoina, R2	-176.3562	56.8360	2294	-3.103	0.1300
Sarge, R1 - Despoina, R3	-740.9733	56.8360	2294	-13.037	<.0001
Sarge, R1 - Despoina, R4	-1096.8269	56.8360	2294	-19.298	<.0001
Sarge, R1 - Queen, R1	-202.2131	56.8360	2294	-3.558	0.0329
Sarge, R1 - Queen, R2	-788.9164	56.8360	2294	-13.881	<.0001
Sarge, R1 - Queen, R3	-1116.7756	56.8360	2294	-19.649	<.0001
Sarge, R1 - Queen, R4	-1159.4556	56.8360	2294	-20.400	<.0001
Sarge, R2 - Sarge, R3	-572.5831	56.8360	2294	-10.074	<.0001
Sarge, R2 - Sarge, R4	-774.7264	56.8360	2294	-13.631	<.0001
Sarge, R2 - Despoina, R1	378.1833	56.8360	2294	6.654	<.0001
Sarge, R2 - Despoina, R2	136.2038	56.8360	2294	2.396	0.5505
Sarge, R2 - Despoina, R3	-428.4133	56.8360	2294	-7.538	<.0001
Sarge, R2 - Despoina, R4	-784.2669	56.8360	2294	-13.799	<.0001
Sarge, R2 - Queen, R1	110.3469	56.8360	2294	1.941	0.8564
Sarge, R2 - Queen, R2	-476.3564	56.8360	2294	-8.381	<.0001
Sarge, R2 - Queen, R3	-804.2156	56.8360	2294	-14.150	<.0001
Sarge, R2 - Queen, R4	-846.8956	56.8360	2294	-14.901	<.0001
Sarge, R3 - Sarge, R4	-202.1433	56.8360	2294	-3.557	0.0331
Sarge, R3 - Despoina, R1	950.7664	56.8360	2294	16.728	<.0001
Sarge, R3 - Despoina, R2	708.7869	56.8360	2294	12.471	<.0001
Sarge, R3 - Despoina, R3	144.1697	56.8360	2294	2.537	0.4447
Sarge, R3 - Despoina, R4	-211.6838	56.8360	2294	-3.724	0.0185
Sarge, R3 - Queen, R1	682.9300	56.8360	2294	12.016	<.0001
Sarge, R3 - Queen, R2	96.2267	56.8360	2294	1.693	0.9489
Sarge, R3 - Queen, R3	-231.6326	56.8360	2294	-4.075	0.0048
Sarge, R3 - Queen, R4	-274.3126	56.8360	2294	-4.826	0.0002
Sarge, R4 - Despoina, R1	1152.9097	56.8360	2294	20.285	<.0001
Sarge, R4 - Despoina, R2	910.9303	56.8360	2294	16.027	<.0001
Sarge, R4 - Despoina, R3	346.3131	56.8360	2294	6.093	<.0001
Sarge, R4 - Despoina, R4	-9.5405	56.8360	2294	-0.168	1.0000
Sarge, R4 - Queen, R1	885.0733	56.8360	2294	15.572	<.0001
Sarge, R4 - Queen, R2	298.3700	56.8360	2294	5.250	<.0001
Sarge, R4 - Queen, R3	-29.4892	56.8360	2294	-0.519	1.0000
Sarge, R4 - Queen, R4	-72.1692	56.8360	2294	-1.270	0.9968
Despoina, R1 - Despoina, R2	-241.9795	56.8360	2294	-4.258	0.0023

Table 7 – *Continued from previous page*

contrast	estimate	SE	df	t.ratio	p.value
Despoina, R1 - Despoina, R3	-806.5967	56.8360	2294	-14.192	<.0001
Despoina, R1 - Despoina, R4	-1162.4503	56.8360	2294	-20.453	<.0001
Despoina, R1 - Queen, R1	-267.8364	56.8360	2294	-4.712	0.0003
Despoina, R1 - Queen, R2	-854.5397	56.8360	2294	-15.035	<.0001
Despoina, R1 - Queen, R3	-1182.3990	56.8360	2294	-20.804	<.0001
Despoina, R1 - Queen, R4	-1225.0790	56.8360	2294	-21.555	<.0001
Despoina, R2 - Despoina, R3	-564.6172	56.8360	2294	-9.934	<.0001
Despoina, R2 - Despoina, R4	-920.4708	56.8360	2294	-16.195	<.0001
Despoina, R2 - Queen, R1	-25.8569	56.8360	2294	-0.455	1.0000
Despoina, R2 - Queen, R2	-612.5603	56.8360	2294	-10.778	<.0001
Despoina, R2 - Queen, R3	-940.4195	56.8360	2294	-16.546	<.0001
Despoina, R2 - Queen, R4	-983.0995	56.8360	2294	-17.297	<.0001
Despoina, R3 - Despoina, R4	-355.8536	56.8360	2294	-6.261	<.0001
Despoina, R3 - Queen, R1	538.7603	56.8360	2294	9.479	<.0001
Despoina, R3 - Queen, R2	-47.9431	56.8360	2294	-0.844	1.0000
Despoina, R3 - Queen, R3	-375.8023	56.8360	2294	-6.612	<.0001
Despoina, R3 - Queen, R4	-418.4823	56.8360	2294	-7.363	<.0001
Despoina, R4 - Queen, R1	894.6138	56.8360	2294	15.740	<.0001
Despoina, R4 - Queen, R2	307.9105	56.8360	2294	5.418	<.0001
Despoina, R4 - Queen, R3	-19.9487	56.8360	2294	-0.351	1.0000
Despoina, R4 - Queen, R4	-62.6287	56.8360	2294	-1.102	0.9994
Queen, R1 - Queen, R2	-586.7033	56.8360	2294	-10.323	<.0001
Queen, R1 - Queen, R3	-914.5626	56.8360	2294	-16.091	<.0001
Queen, R1 - Queen, R4	-957.2426	56.8360	2294	-16.842	<.0001
Queen, R2 - Queen, R3	-327.8592	56.8360	2294	-5.769	<.0001
Queen, R2 - Queen, R4	-370.5392	56.8360	2294	-6.519	<.0001
Queen, R3 - Queen, R4	-42.6800	56.8360	2294	-0.751	1.0000

Results are averaged over the levels of: DoF, Codecs

Degrees-of-freedom method: kenward-roger

P value adjustment: tukey method for comparing a family of 16 estimates

Table 8: Contrast test between factors Content, Codec and Bitrate

contrast	estimate	SE	df	t.ratio	p.value
Longdress, C1, R1 - Longdress, C1, R2	-535.4682	70.4123	2263	-7.605	<.0001
Longdress, C1, R1 - Longdress, C1, R3	-619.6446	70.4123	2263	-8.800	<.0001
Longdress, C1, R1 - Longdress, C1, R4	-657.2754	70.4123	2263	-9.335	<.0001
Longdress, C1, R1 - Longdress, C2, R1	636.6415	70.4123	2263	9.042	<.0001
Longdress, C1, R1 - Longdress, C2, R2	328.2036	70.4123	2263	4.661	0.0015
Longdress, C1, R1 - Longdress, C2, R3	-242.6631	70.4123	2263	-3.446	0.1438
Longdress, C1, R1 - Longdress, C2, R4	-507.2836	70.4123	2263	-7.204	<.0001
Longdress, C1, R1 - Loot, C1, R1	446.7518	70.4123	2263	6.345	<.0001
Longdress, C1, R1 - Loot, C1, R2	-224.4031	70.4123	2263	-3.187	0.2794
Longdress, C1, R1 - Loot, C1, R3	-467.3159	70.4123	2263	-6.637	<.0001
Longdress, C1, R1 - Loot, C1, R4	-535.5154	70.4123	2263	-7.605	<.0001
Longdress, C1, R1 - Loot, C2, R1	1014.3595	70.4123	2263	14.406	<.0001
Longdress, C1, R1 - Loot, C2, R2	799.7723	70.4123	2263	11.358	<.0001
Longdress, C1, R1 - Loot, C2, R3	343.0297	70.4123	2263	4.872	0.0005
Longdress, C1, R1 - Loot, C2, R4	-247.0190	70.4123	2263	-3.508	0.1204
Longdress, C1, R1 - Red and black, C1, R1	193.1303	70.4123	2263	2.743	0.6257
Longdress, C1, R1 - Red and black, C1, R2	-301.1995	70.4123	2263	-4.278	0.0078

Table 8 – *Continued from previous page*

contrast	estimate	SE	df	t.ratio	p.value
Longdress, C1, R1 - Red and black, C1, R3	-537.7385	70.4123	2263	-7.637	<.0001
Longdress, C1, R1 - Red and black, C1, R4	-565.3785	70.4123	2263	-8.030	<.0001
Longdress, C1, R1 - Red and black, C2, R1	746.5923	70.4123	2263	10.603	<.0001
Longdress, C1, R1 - Red and black, C2, R2	459.9036	70.4123	2263	6.532	<.0001
Longdress, C1, R1 - Red and black, C2, R3	43.6846	70.4123	2263	0.620	1.0000
Longdress, C1, R1 - Red and black, C2, R4	-297.4928	70.4123	2263	-4.225	0.0097
Longdress, C1, R1 - Soldier, C1, R1	760.3185	70.4123	2263	10.798	<.0001
Longdress, C1, R1 - Soldier, C1, R2	150.9123	70.4123	2263	2.143	0.9611
Longdress, C1, R1 - Soldier, C1, R3	-281.4026	70.4123	2263	-3.996	0.0235
Longdress, C1, R1 - Soldier, C1, R4	-472.6487	70.4123	2263	-6.713	<.0001
Longdress, C1, R1 - Soldier, C2, R1	1057.4472	70.4123	2263	15.018	<.0001
Longdress, C1, R1 - Soldier, C2, R2	842.4862	70.4123	2263	11.965	<.0001
Longdress, C1, R1 - Soldier, C2, R3	403.9667	70.4123	2263	5.737	<.0001
Longdress, C1, R1 - Soldier, C2, R4	-217.4087	70.4123	2263	-3.088	0.3475
Longdress, C1, R2 - Longdress, C1, R3	-84.1764	70.4123	2263	-1.195	1.0000
Longdress, C1, R2 - Longdress, C1, R4	-121.8072	70.4123	2263	-1.730	0.9984
Longdress, C1, R2 - Longdress, C2, R1	1172.1097	70.4123	2263	16.646	<.0001
Longdress, C1, R2 - Longdress, C2, R2	863.6718	70.4123	2263	12.266	<.0001
Longdress, C1, R2 - Longdress, C2, R3	292.8051	70.4123	2263	4.158	0.0126
Longdress, C1, R2 - Longdress, C2, R4	28.1846	70.4123	2263	0.400	1.0000
Longdress, C1, R2 - Loot, C1, R1	982.2200	70.4123	2263	13.950	<.0001
Longdress, C1, R2 - Loot, C1, R2	311.0651	70.4123	2263	4.418	0.0043
Longdress, C1, R2 - Loot, C1, R3	68.1523	70.4123	2263	0.968	1.0000
Longdress, C1, R2 - Loot, C1, R4	-0.0472	70.4123	2263	-0.001	1.0000
Longdress, C1, R2 - Loot, C2, R1	1549.8277	70.4123	2263	22.011	<.0001
Longdress, C1, R2 - Loot, C2, R2	1335.2405	70.4123	2263	18.963	<.0001
Longdress, C1, R2 - Loot, C2, R3	878.4979	70.4123	2263	12.476	<.0001
Longdress, C1, R2 - Loot, C2, R4	288.4492	70.4123	2263	4.097	0.0161
Longdress, C1, R2 - Red and black, C1, R1	728.5985	70.4123	2263	10.348	<.0001
Longdress, C1, R2 - Red and black, C1, R2	234.2687	70.4123	2263	3.327	0.1984
Longdress, C1, R2 - Red and black, C1, R3	-2.2703	70.4123	2263	-0.032	1.0000
Longdress, C1, R2 - Red and black, C1, R4	-29.9103	70.4123	2263	-0.425	1.0000
Longdress, C1, R2 - Red and black, C2, R1	1282.0605	70.4123	2263	18.208	<.0001
Longdress, C1, R2 - Red and black, C2, R2	995.3718	70.4123	2263	14.136	<.0001
Longdress, C1, R2 - Red and black, C2, R3	579.1528	70.4123	2263	8.225	<.0001
Longdress, C1, R2 - Red and black, C2, R4	237.9754	70.4123	2263	3.380	0.1727
Longdress, C1, R2 - Soldier, C1, R1	1295.7867	70.4123	2263	18.403	<.0001
Longdress, C1, R2 - Soldier, C1, R2	686.3805	70.4123	2263	9.748	<.0001
Longdress, C1, R2 - Soldier, C1, R3	254.0656	70.4123	2263	3.608	0.0890
Longdress, C1, R2 - Soldier, C1, R4	62.8195	70.4123	2263	0.892	1.0000
Longdress, C1, R2 - Soldier, C2, R1	1592.9154	70.4123	2263	22.623	<.0001
Longdress, C1, R2 - Soldier, C2, R2	1377.9544	70.4123	2263	19.570	<.0001
Longdress, C1, R2 - Soldier, C2, R3	939.4349	70.4123	2263	13.342	<.0001
Longdress, C1, R2 - Soldier, C2, R4	318.0595	70.4123	2263	4.517	0.0028
Longdress, C1, R3 - Longdress, C1, R4	-37.6308	70.4123	2263	-0.534	1.0000
Longdress, C1, R3 - Longdress, C2, R1	1256.2862	70.4123	2263	17.842	<.0001
Longdress, C1, R3 - Longdress, C2, R2	947.8482	70.4123	2263	13.461	<.0001
Longdress, C1, R3 - Longdress, C2, R3	376.9815	70.4123	2263	5.354	<.0001
Longdress, C1, R3 - Longdress, C2, R4	112.3610	70.4123	2263	1.596	0.9996
Longdress, C1, R3 - Loot, C1, R1	1066.3964	70.4123	2263	15.145	<.0001
Longdress, C1, R3 - Loot, C1, R2	395.2415	70.4123	2263	5.613	<.0001

Table 8 – *Continued from previous page*

contrast	estimate	SE	df	t.ratio	p.value
Longdress, C1, R3 - Loot, C1, R3	152.3287	70.4123	2263	2.163	0.9564
Longdress, C1, R3 - Loot, C1, R4	84.1292	70.4123	2263	1.195	1.0000
Longdress, C1, R3 - Loot, C2, R1	1634.0041	70.4123	2263	23.206	<.0001
Longdress, C1, R3 - Loot, C2, R2	1419.4169	70.4123	2263	20.159	<.0001
Longdress, C1, R3 - Loot, C2, R3	962.6744	70.4123	2263	13.672	<.0001
Longdress, C1, R3 - Loot, C2, R4	372.6256	70.4123	2263	5.292	0.0001
Longdress, C1, R3 - Red and black, C1, R1	812.7749	70.4123	2263	11.543	<.0001
Longdress, C1, R3 - Red and black, C1, R2	318.4451	70.4123	2263	4.523	0.0027
Longdress, C1, R3 - Red and black, C1, R3	81.9062	70.4123	2263	1.163	1.0000
Longdress, C1, R3 - Red and black, C1, R4	54.2662	70.4123	2263	0.771	1.0000
Longdress, C1, R3 - Red and black, C2, R1	1366.2369	70.4123	2263	19.403	<.0001
Longdress, C1, R3 - Red and black, C2, R2	1079.5482	70.4123	2263	15.332	<.0001
Longdress, C1, R3 - Red and black, C2, R3	663.3292	70.4123	2263	9.421	<.0001
Longdress, C1, R3 - Red and black, C2, R4	322.1518	70.4123	2263	4.575	0.0021
Longdress, C1, R3 - Soldier, C1, R1	1379.9631	70.4123	2263	19.598	<.0001
Longdress, C1, R3 - Soldier, C1, R2	770.5569	70.4123	2263	10.944	<.0001
Longdress, C1, R3 - Soldier, C1, R3	338.2421	70.4123	2263	4.804	0.0007
Longdress, C1, R3 - Soldier, C1, R4	146.9959	70.4123	2263	2.088	0.9721
Longdress, C1, R3 - Soldier, C2, R1	1677.0918	70.4123	2263	23.818	<.0001
Longdress, C1, R3 - Soldier, C2, R2	1462.1308	70.4123	2263	20.765	<.0001
Longdress, C1, R3 - Soldier, C2, R3	1023.6113	70.4123	2263	14.537	<.0001
Longdress, C1, R3 - Soldier, C2, R4	402.2359	70.4123	2263	5.713	<.0001
Longdress, C1, R4 - Longdress, C2, R1	1293.9169	70.4123	2263	18.376	<.0001
Longdress, C1, R4 - Longdress, C2, R2	985.4790	70.4123	2263	13.996	<.0001
Longdress, C1, R4 - Longdress, C2, R3	414.6123	70.4123	2263	5.888	<.0001
Longdress, C1, R4 - Longdress, C2, R4	149.9918	70.4123	2263	2.130	0.9639
Longdress, C1, R4 - Loot, C1, R1	1104.0272	70.4123	2263	15.679	<.0001
Longdress, C1, R4 - Loot, C1, R2	432.8723	70.4123	2263	6.148	<.0001
Longdress, C1, R4 - Loot, C1, R3	189.9595	70.4123	2263	2.698	0.6625
Longdress, C1, R4 - Loot, C1, R4	121.7600	70.4123	2263	1.729	0.9984
Longdress, C1, R4 - Loot, C2, R1	1671.6349	70.4123	2263	23.741	<.0001
Longdress, C1, R4 - Loot, C2, R2	1457.0477	70.4123	2263	20.693	<.0001
Longdress, C1, R4 - Loot, C2, R3	1000.3051	70.4123	2263	14.206	<.0001
Longdress, C1, R4 - Loot, C2, R4	410.2564	70.4123	2263	5.826	<.0001
Longdress, C1, R4 - Red and black, C1, R1	850.4056	70.4123	2263	12.078	<.0001
Longdress, C1, R4 - Red and black, C1, R2	356.0759	70.4123	2263	5.057	0.0002
Longdress, C1, R4 - Red and black, C1, R3	119.5369	70.4123	2263	1.698	0.9989
Longdress, C1, R4 - Red and black, C1, R4	91.8969	70.4123	2263	1.305	1.0000
Longdress, C1, R4 - Red and black, C2, R1	1403.8677	70.4123	2263	19.938	<.0001
Longdress, C1, R4 - Red and black, C2, R2	1117.1790	70.4123	2263	15.866	<.0001
Longdress, C1, R4 - Red and black, C2, R3	700.9600	70.4123	2263	9.955	<.0001
Longdress, C1, R4 - Red and black, C2, R4	359.7826	70.4123	2263	5.110	0.0002
Longdress, C1, R4 - Soldier, C1, R1	1417.5938	70.4123	2263	20.133	<.0001
Longdress, C1, R4 - Soldier, C1, R2	808.1877	70.4123	2263	11.478	<.0001
Longdress, C1, R4 - Soldier, C1, R3	375.8728	70.4123	2263	5.338	<.0001
Longdress, C1, R4 - Soldier, C1, R4	184.6267	70.4123	2263	2.622	0.7219
Longdress, C1, R4 - Soldier, C2, R1	1714.7226	70.4123	2263	24.353	<.0001
Longdress, C1, R4 - Soldier, C2, R2	1499.7615	70.4123	2263	21.300	<.0001
Longdress, C1, R4 - Soldier, C2, R3	1061.2421	70.4123	2263	15.072	<.0001
Longdress, C1, R4 - Soldier, C2, R4	439.8667	70.4123	2263	6.247	<.0001
Longdress, C2, R1 - Longdress, C2, R2	-308.4379	70.4123	2263	-4.380	0.0051

Table 8 – *Continued from previous page*

contrast	estimate	SE	df	t.ratio	p.value
Longdress, C2, R1 - Longdress, C2, R3	-879.3046	70.4123	2263	-12.488	<.0001
Longdress, C2, R1 - Longdress, C2, R4	-1143.9251	70.4123	2263	-16.246	<.0001
Longdress, C2, R1 - Loot, C1, R1	-189.8897	70.4123	2263	-2.697	0.6633
Longdress, C2, R1 - Loot, C1, R2	-861.0446	70.4123	2263	-12.229	<.0001
Longdress, C2, R1 - Loot, C1, R3	-1103.9574	70.4123	2263	-15.678	<.0001
Longdress, C2, R1 - Loot, C1, R4	-1172.1569	70.4123	2263	-16.647	<.0001
Longdress, C2, R1 - Loot, C2, R1	377.7179	70.4123	2263	5.364	<.0001
Longdress, C2, R1 - Loot, C2, R2	163.1308	70.4123	2263	2.317	0.9058
Longdress, C2, R1 - Loot, C2, R3	-293.6118	70.4123	2263	-4.170	0.0120
Longdress, C2, R1 - Loot, C2, R4	-883.6605	70.4123	2263	-12.550	<.0001
Longdress, C2, R1 - Red and black, C1, R1	-443.5113	70.4123	2263	-6.299	<.0001
Longdress, C2, R1 - Red and black, C1, R2	-937.8410	70.4123	2263	-13.319	<.0001
Longdress, C2, R1 - Red and black, C1, R3	-1174.3800	70.4123	2263	-16.679	<.0001
Longdress, C2, R1 - Red and black, C1, R4	-1202.0200	70.4123	2263	-17.071	<.0001
Longdress, C2, R1 - Red and black, C2, R1	109.9508	70.4123	2263	1.562	0.9998
Longdress, C2, R1 - Red and black, C2, R2	-176.7379	70.4123	2263	-2.510	0.8014
Longdress, C2, R1 - Red and black, C2, R3	-592.9569	70.4123	2263	-8.421	<.0001
Longdress, C2, R1 - Red and black, C2, R4	-934.1344	70.4123	2263	-13.267	<.0001
Longdress, C2, R1 - Soldier, C1, R1	123.6769	70.4123	2263	1.756	0.9979
Longdress, C2, R1 - Soldier, C1, R2	-485.7292	70.4123	2263	-6.898	<.0001
Longdress, C2, R1 - Soldier, C1, R3	-918.0441	70.4123	2263	-13.038	<.0001
Longdress, C2, R1 - Soldier, C1, R4	-1109.2903	70.4123	2263	-15.754	<.0001
Longdress, C2, R1 - Soldier, C2, R1	420.8056	70.4123	2263	5.976	<.0001
Longdress, C2, R1 - Soldier, C2, R2	205.8446	70.4123	2263	2.923	0.4754
Longdress, C2, R1 - Soldier, C2, R3	-232.6749	70.4123	2263	-3.304	0.2103
Longdress, C2, R1 - Soldier, C2, R4	-854.0503	70.4123	2263	-12.129	<.0001
Longdress, C2, R2 - Longdress, C2, R3	-570.8667	70.4123	2263	-8.107	<.0001
Longdress, C2, R2 - Longdress, C2, R4	-835.4872	70.4123	2263	-11.866	<.0001
Longdress, C2, R2 - Loot, C1, R1	118.5482	70.4123	2263	1.684	0.9990
Longdress, C2, R2 - Loot, C1, R2	-552.6067	70.4123	2263	-7.848	<.0001
Longdress, C2, R2 - Loot, C1, R3	-795.5195	70.4123	2263	-11.298	<.0001
Longdress, C2, R2 - Loot, C1, R4	-863.7190	70.4123	2263	-12.267	<.0001
Longdress, C2, R2 - Loot, C2, R1	686.1559	70.4123	2263	9.745	<.0001
Longdress, C2, R2 - Loot, C2, R2	471.5687	70.4123	2263	6.697	<.0001
Longdress, C2, R2 - Loot, C2, R3	14.8262	70.4123	2263	0.211	1.0000
Longdress, C2, R2 - Loot, C2, R4	-575.2226	70.4123	2263	-8.169	<.0001
Longdress, C2, R2 - Red and black, C1, R1	-135.0733	70.4123	2263	-1.918	0.9915
Longdress, C2, R2 - Red and black, C1, R2	-629.4031	70.4123	2263	-8.939	<.0001
Longdress, C2, R2 - Red and black, C1, R3	-865.9421	70.4123	2263	-12.298	<.0001
Longdress, C2, R2 - Red and black, C1, R4	-893.5821	70.4123	2263	-12.691	<.0001
Longdress, C2, R2 - Red and black, C2, R1	418.3887	70.4123	2263	5.942	<.0001
Longdress, C2, R2 - Red and black, C2, R2	131.7000	70.4123	2263	1.870	0.9942
Longdress, C2, R2 - Red and black, C2, R3	-284.5190	70.4123	2263	-4.041	0.0199
Longdress, C2, R2 - Red and black, C2, R4	-625.6964	70.4123	2263	-8.886	<.0001
Longdress, C2, R2 - Soldier, C1, R1	432.1149	70.4123	2263	6.137	<.0001
Longdress, C2, R2 - Soldier, C1, R2	-177.2913	70.4123	2263	-2.518	0.7962
Longdress, C2, R2 - Soldier, C1, R3	-609.6062	70.4123	2263	-8.658	<.0001
Longdress, C2, R2 - Soldier, C1, R4	-800.8523	70.4123	2263	-11.374	<.0001
Longdress, C2, R2 - Soldier, C2, R1	729.2436	70.4123	2263	10.357	<.0001
Longdress, C2, R2 - Soldier, C2, R2	514.2826	70.4123	2263	7.304	<.0001
Longdress, C2, R2 - Soldier, C2, R3	75.7631	70.4123	2263	1.076	1.0000

Table 8 – *Continued from previous page*

contrast	estimate	SE	df	t.ratio	p.value
Longdress, C2, R2 - Soldier, C2, R4	-545.6123	70.4123	2263	-7.749	<.0001
Longdress, C2, R3 - Longdress, C2, R4	-264.6205	70.4123	2263	-3.758	0.0548
Longdress, C2, R3 - Loot, C1, R1	689.4149	70.4123	2263	9.791	<.0001
Longdress, C2, R3 - Loot, C1, R2	18.2600	70.4123	2263	0.259	1.0000
Longdress, C2, R3 - Loot, C1, R3	-224.6528	70.4123	2263	-3.191	0.2771
Longdress, C2, R3 - Loot, C1, R4	-292.8523	70.4123	2263	-4.159	0.0126
Longdress, C2, R3 - Loot, C2, R1	1257.0226	70.4123	2263	17.852	<.0001
Longdress, C2, R3 - Loot, C2, R2	1042.4354	70.4123	2263	14.805	<.0001
Longdress, C2, R3 - Loot, C2, R3	585.6928	70.4123	2263	8.318	<.0001
Longdress, C2, R3 - Loot, C2, R4	-4.3559	70.4123	2263	-0.062	1.0000
Longdress, C2, R3 - Red and black, C1, R1	435.7933	70.4123	2263	6.189	<.0001
Longdress, C2, R3 - Red and black, C1, R2	-58.5364	70.4123	2263	-0.831	1.0000
Longdress, C2, R3 - Red and black, C1, R3	-295.0754	70.4123	2263	-4.191	0.0111
Longdress, C2, R3 - Red and black, C1, R4	-322.7154	70.4123	2263	-4.583	0.0021
Longdress, C2, R3 - Red and black, C2, R1	989.2554	70.4123	2263	14.049	<.0001
Longdress, C2, R3 - Red and black, C2, R2	702.5667	70.4123	2263	9.978	<.0001
Longdress, C2, R3 - Red and black, C2, R3	286.3477	70.4123	2263	4.067	0.0180
Longdress, C2, R3 - Red and black, C2, R4	-54.8297	70.4123	2263	-0.779	1.0000
Longdress, C2, R3 - Soldier, C1, R1	1002.9815	70.4123	2263	14.244	<.0001
Longdress, C2, R3 - Soldier, C1, R2	393.5754	70.4123	2263	5.590	<.0001
Longdress, C2, R3 - Soldier, C1, R3	-38.7395	70.4123	2263	-0.550	1.0000
Longdress, C2, R3 - Soldier, C1, R4	-229.9856	70.4123	2263	-3.266	0.2313
Longdress, C2, R3 - Soldier, C2, R1	1300.1103	70.4123	2263	18.464	<.0001
Longdress, C2, R3 - Soldier, C2, R2	1085.1492	70.4123	2263	15.411	<.0001
Longdress, C2, R3 - Soldier, C2, R3	646.6297	70.4123	2263	9.183	<.0001
Longdress, C2, R3 - Soldier, C2, R4	25.2544	70.4123	2263	0.359	1.0000
Longdress, C2, R4 - Loot, C1, R1	954.0354	70.4123	2263	13.549	<.0001
Longdress, C2, R4 - Loot, C1, R2	282.8805	70.4123	2263	4.017	0.0217
Longdress, C2, R4 - Loot, C1, R3	39.9677	70.4123	2263	0.568	1.0000
Longdress, C2, R4 - Loot, C1, R4	-28.2318	70.4123	2263	-0.401	1.0000
Longdress, C2, R4 - Loot, C2, R1	1521.6431	70.4123	2263	21.610	<.0001
Longdress, C2, R4 - Loot, C2, R2	1307.0559	70.4123	2263	18.563	<.0001
Longdress, C2, R4 - Loot, C2, R3	850.3133	70.4123	2263	12.076	<.0001
Longdress, C2, R4 - Loot, C2, R4	260.2646	70.4123	2263	3.696	0.0673
Longdress, C2, R4 - Red and black, C1, R1	700.4138	70.4123	2263	9.947	<.0001
Longdress, C2, R4 - Red and black, C1, R2	206.0841	70.4123	2263	2.927	0.4726
Longdress, C2, R4 - Red and black, C1, R3	-30.4549	70.4123	2263	-0.433	1.0000
Longdress, C2, R4 - Red and black, C1, R4	-58.0949	70.4123	2263	-0.825	1.0000
Longdress, C2, R4 - Red and black, C2, R1	1253.8759	70.4123	2263	17.808	<.0001
Longdress, C2, R4 - Red and black, C2, R2	967.1872	70.4123	2263	13.736	<.0001
Longdress, C2, R4 - Red and black, C2, R3	550.9682	70.4123	2263	7.825	<.0001
Longdress, C2, R4 - Red and black, C2, R4	209.7908	70.4123	2263	2.979	0.4300
Longdress, C2, R4 - Soldier, C1, R1	1267.6021	70.4123	2263	18.003	<.0001
Longdress, C2, R4 - Soldier, C1, R2	658.1959	70.4123	2263	9.348	<.0001
Longdress, C2, R4 - Soldier, C1, R3	225.8810	70.4123	2263	3.208	0.2661
Longdress, C2, R4 - Soldier, C1, R4	34.6349	70.4123	2263	0.492	1.0000
Longdress, C2, R4 - Soldier, C2, R1	1564.7308	70.4123	2263	22.222	<.0001
Longdress, C2, R4 - Soldier, C2, R2	1349.7697	70.4123	2263	19.170	<.0001
Longdress, C2, R4 - Soldier, C2, R3	911.2503	70.4123	2263	12.942	<.0001
Longdress, C2, R4 - Soldier, C2, R4	289.8749	70.4123	2263	4.117	0.0149
Loot, C1, R1 - Loot, C1, R2	-671.1549	70.4123	2263	-9.532	<.0001

Table 8 – *Continued from previous page*

contrast	estimate	SE	df	t.ratio	p.value
Loot, C1, R1 - Loot, C1, R3	-914.0677	70.4123	2263	-12.982	<.0001
Loot, C1, R1 - Loot, C1, R4	-982.2672	70.4123	2263	-13.950	<.0001
Loot, C1, R1 - Loot, C2, R1	567.6077	70.4123	2263	8.061	<.0001
Loot, C1, R1 - Loot, C2, R2	353.0205	70.4123	2263	5.014	0.0003
Loot, C1, R1 - Loot, C2, R3	-103.7221	70.4123	2263	-1.473	0.9999
Loot, C1, R1 - Loot, C2, R4	-693.7708	70.4123	2263	-9.853	<.0001
Loot, C1, R1 - Red and black, C1, R1	-253.6215	70.4123	2263	-3.602	0.0908
Loot, C1, R1 - Red and black, C1, R2	-747.9513	70.4123	2263	-10.622	<.0001
Loot, C1, R1 - Red and black, C1, R3	-984.4903	70.4123	2263	-13.982	<.0001
Loot, C1, R1 - Red and black, C1, R4	-1012.1303	70.4123	2263	-14.374	<.0001
Loot, C1, R1 - Red and black, C2, R1	299.8405	70.4123	2263	4.258	0.0084
Loot, C1, R1 - Red and black, C2, R2	13.1518	70.4123	2263	0.187	1.0000
Loot, C1, R1 - Red and black, C2, R3	-403.0672	70.4123	2263	-5.724	<.0001
Loot, C1, R1 - Red and black, C2, R4	-744.2446	70.4123	2263	-10.570	<.0001
Loot, C1, R1 - Soldier, C1, R1	313.5667	70.4123	2263	4.453	0.0037
Loot, C1, R1 - Soldier, C1, R2	-295.8395	70.4123	2263	-4.202	0.0106
Loot, C1, R1 - Soldier, C1, R3	-728.1544	70.4123	2263	-10.341	<.0001
Loot, C1, R1 - Soldier, C1, R4	-919.4005	70.4123	2263	-13.057	<.0001
Loot, C1, R1 - Soldier, C2, R1	610.6954	70.4123	2263	8.673	<.0001
Loot, C1, R1 - Soldier, C2, R2	395.7344	70.4123	2263	5.620	<.0001
Loot, C1, R1 - Soldier, C2, R3	-42.7851	70.4123	2263	-0.608	1.0000
Loot, C1, R1 - Soldier, C2, R4	-664.1605	70.4123	2263	-9.432	<.0001
Loot, C1, R2 - Loot, C1, R3	-242.9128	70.4123	2263	-3.450	0.1424
Loot, C1, R2 - Loot, C1, R4	-311.1123	70.4123	2263	-4.418	0.0043
Loot, C1, R2 - Loot, C2, R1	1238.7626	70.4123	2263	17.593	<.0001
Loot, C1, R2 - Loot, C2, R2	1024.1754	70.4123	2263	14.545	<.0001
Loot, C1, R2 - Loot, C2, R3	567.4328	70.4123	2263	8.059	<.0001
Loot, C1, R2 - Loot, C2, R4	-22.6159	70.4123	2263	-0.321	1.0000
Loot, C1, R2 - Red and black, C1, R1	417.5333	70.4123	2263	5.930	<.0001
Loot, C1, R2 - Red and black, C1, R2	-76.7964	70.4123	2263	-1.091	1.0000
Loot, C1, R2 - Red and black, C1, R3	-313.3354	70.4123	2263	-4.450	0.0037
Loot, C1, R2 - Red and black, C1, R4	-340.9754	70.4123	2263	-4.843	0.0006
Loot, C1, R2 - Red and black, C2, R1	970.9954	70.4123	2263	13.790	<.0001
Loot, C1, R2 - Red and black, C2, R2	684.3067	70.4123	2263	9.719	<.0001
Loot, C1, R2 - Red and black, C2, R3	268.0877	70.4123	2263	3.807	0.0464
Loot, C1, R2 - Red and black, C2, R4	-73.0897	70.4123	2263	-1.038	1.0000
Loot, C1, R2 - Soldier, C1, R1	984.7215	70.4123	2263	13.985	<.0001
Loot, C1, R2 - Soldier, C1, R2	375.3154	70.4123	2263	5.330	0.0001
Loot, C1, R2 - Soldier, C1, R3	-56.9995	70.4123	2263	-0.810	1.0000
Loot, C1, R2 - Soldier, C1, R4	-248.2456	70.4123	2263	-3.526	0.1144
Loot, C1, R2 - Soldier, C2, R1	1281.8503	70.4123	2263	18.205	<.0001
Loot, C1, R2 - Soldier, C2, R2	1066.8892	70.4123	2263	15.152	<.0001
Loot, C1, R2 - Soldier, C2, R3	628.3697	70.4123	2263	8.924	<.0001
Loot, C1, R2 - Soldier, C2, R4	6.9944	70.4123	2263	0.099	1.0000
Loot, C1, R3 - Loot, C1, R4	-68.1995	70.4123	2263	-0.969	1.0000
Loot, C1, R3 - Loot, C2, R1	1481.6754	70.4123	2263	21.043	<.0001
Loot, C1, R3 - Loot, C2, R2	1267.0882	70.4123	2263	17.995	<.0001
Loot, C1, R3 - Loot, C2, R3	810.3456	70.4123	2263	11.509	<.0001
Loot, C1, R3 - Loot, C2, R4	220.2969	70.4123	2263	3.129	0.3184
Loot, C1, R3 - Red and black, C1, R1	660.4462	70.4123	2263	9.380	<.0001
Loot, C1, R3 - Red and black, C1, R2	166.1164	70.4123	2263	2.359	0.8868

Table 8 – *Continued from previous page*

contrast	estimate	SE	df	t.ratio	p.value
Loot, C1, R3 - Red and black, C1, R3	-70.4226	70.4123	2263	-1.000	1.0000
Loot, C1, R3 - Red and black, C1, R4	-98.0626	70.4123	2263	-1.393	1.0000
Loot, C1, R3 - Red and black, C2, R1	1213.9082	70.4123	2263	17.240	<.0001
Loot, C1, R3 - Red and black, C2, R2	927.2195	70.4123	2263	13.168	<.0001
Loot, C1, R3 - Red and black, C2, R3	511.0005	70.4123	2263	7.257	<.0001
Loot, C1, R3 - Red and black, C2, R4	169.8231	70.4123	2263	2.412	0.8601
Loot, C1, R3 - Soldier, C1, R1	1227.6344	70.4123	2263	17.435	<.0001
Loot, C1, R3 - Soldier, C1, R2	618.2282	70.4123	2263	8.780	<.0001
Loot, C1, R3 - Soldier, C1, R3	185.9133	70.4123	2263	2.640	0.7079
Loot, C1, R3 - Soldier, C1, R4	-5.3328	70.4123	2263	-0.076	1.0000
Loot, C1, R3 - Soldier, C2, R1	1524.7631	70.4123	2263	21.655	<.0001
Loot, C1, R3 - Soldier, C2, R2	1309.8021	70.4123	2263	18.602	<.0001
Loot, C1, R3 - Soldier, C2, R3	871.2826	70.4123	2263	12.374	<.0001
Loot, C1, R3 - Soldier, C2, R4	249.9072	70.4123	2263	3.549	0.1066
Loot, C1, R4 - Loot, C2, R1	1549.8749	70.4123	2263	22.011	<.0001
Loot, C1, R4 - Loot, C2, R2	1335.2877	70.4123	2263	18.964	<.0001
Loot, C1, R4 - Loot, C2, R3	878.5451	70.4123	2263	12.477	<.0001
Loot, C1, R4 - Loot, C2, R4	288.4964	70.4123	2263	4.097	0.0160
Loot, C1, R4 - Red and black, C1, R1	728.6456	70.4123	2263	10.348	<.0001
Loot, C1, R4 - Red and black, C1, R2	234.3159	70.4123	2263	3.328	0.1981
Loot, C1, R4 - Red and black, C1, R3	-2.2231	70.4123	2263	-0.032	1.0000
Loot, C1, R4 - Red and black, C1, R4	-29.8631	70.4123	2263	-0.424	1.0000
Loot, C1, R4 - Red and black, C2, R1	1282.1077	70.4123	2263	18.209	<.0001
Loot, C1, R4 - Red and black, C2, R2	995.4190	70.4123	2263	14.137	<.0001
Loot, C1, R4 - Red and black, C2, R3	579.2000	70.4123	2263	8.226	<.0001
Loot, C1, R4 - Red and black, C2, R4	238.0226	70.4123	2263	3.380	0.1724
Loot, C1, R4 - Soldier, C1, R1	1295.8338	70.4123	2263	18.404	<.0001
Loot, C1, R4 - Soldier, C1, R2	686.4277	70.4123	2263	9.749	<.0001
Loot, C1, R4 - Soldier, C1, R3	254.1128	70.4123	2263	3.609	0.0888
Loot, C1, R4 - Soldier, C1, R4	62.8667	70.4123	2263	0.893	1.0000
Loot, C1, R4 - Soldier, C2, R1	1592.9626	70.4123	2263	22.623	<.0001
Loot, C1, R4 - Soldier, C2, R2	1378.0015	70.4123	2263	19.570	<.0001
Loot, C1, R4 - Soldier, C2, R3	939.4821	70.4123	2263	13.343	<.0001
Loot, C1, R4 - Soldier, C2, R4	318.1067	70.4123	2263	4.518	0.0028
Loot, C2, R1 - Loot, C2, R2	-214.5872	70.4123	2263	-3.048	0.3771
Loot, C2, R1 - Loot, C2, R3	-671.3297	70.4123	2263	-9.534	<.0001
Loot, C2, R1 - Loot, C2, R4	-1261.3785	70.4123	2263	-17.914	<.0001
Loot, C2, R1 - Red and black, C1, R1	-821.2292	70.4123	2263	-11.663	<.0001
Loot, C2, R1 - Red and black, C1, R2	-1315.5590	70.4123	2263	-18.684	<.0001
Loot, C2, R1 - Red and black, C1, R3	-1552.0979	70.4123	2263	-22.043	<.0001
Loot, C2, R1 - Red and black, C1, R4	-1579.7379	70.4123	2263	-22.436	<.0001
Loot, C2, R1 - Red and black, C2, R1	-267.7672	70.4123	2263	-3.803	0.0471
Loot, C2, R1 - Red and black, C2, R2	-554.4559	70.4123	2263	-7.874	<.0001
Loot, C2, R1 - Red and black, C2, R3	-970.6749	70.4123	2263	-13.786	<.0001
Loot, C2, R1 - Red and black, C2, R4	-1311.8523	70.4123	2263	-18.631	<.0001
Loot, C2, R1 - Soldier, C1, R1	-254.0410	70.4123	2263	-3.608	0.0891
Loot, C2, R1 - Soldier, C1, R2	-863.4472	70.4123	2263	-12.263	<.0001
Loot, C2, R1 - Soldier, C1, R3	-1295.7621	70.4123	2263	-18.402	<.0001
Loot, C2, R1 - Soldier, C1, R4	-1487.0082	70.4123	2263	-21.119	<.0001
Loot, C2, R1 - Soldier, C2, R1	43.0877	70.4123	2263	0.612	1.0000
Loot, C2, R1 - Soldier, C2, R2	-171.8733	70.4123	2263	-2.441	0.8439

Table 8 – *Continued from previous page*

contrast	estimate	SE	df	t.ratio	p.value
Loot, C2, R1 - Soldier, C2, R3	-610.3928	70.4123	2263	-8.669	<.0001
Loot, C2, R1 - Soldier, C2, R4	-1231.7682	70.4123	2263	-17.494	<.0001
Loot, C2, R2 - Loot, C2, R3	-456.7426	70.4123	2263	-6.487	<.0001
Loot, C2, R2 - Loot, C2, R4	-1046.7913	70.4123	2263	-14.867	<.0001
Loot, C2, R2 - Red and black, C1, R1	-606.6421	70.4123	2263	-8.616	<.0001
Loot, C2, R2 - Red and black, C1, R2	-1100.9718	70.4123	2263	-15.636	<.0001
Loot, C2, R2 - Red and black, C1, R3	-1337.5108	70.4123	2263	-18.995	<.0001
Loot, C2, R2 - Red and black, C1, R4	-1365.1508	70.4123	2263	-19.388	<.0001
Loot, C2, R2 - Red and black, C2, R1	-53.1800	70.4123	2263	-0.755	1.0000
Loot, C2, R2 - Red and black, C2, R2	-339.8687	70.4123	2263	-4.827	0.0007
Loot, C2, R2 - Red and black, C2, R3	-756.0877	70.4123	2263	-10.738	<.0001
Loot, C2, R2 - Red and black, C2, R4	-1097.2651	70.4123	2263	-15.583	<.0001
Loot, C2, R2 - Soldier, C1, R1	-39.4538	70.4123	2263	-0.560	1.0000
Loot, C2, R2 - Soldier, C1, R2	-648.8600	70.4123	2263	-9.215	<.0001
Loot, C2, R2 - Soldier, C1, R3	-1081.1749	70.4123	2263	-15.355	<.0001
Loot, C2, R2 - Soldier, C1, R4	-1272.4210	70.4123	2263	-18.071	<.0001
Loot, C2, R2 - Soldier, C2, R1	257.6749	70.4123	2263	3.660	0.0757
Loot, C2, R2 - Soldier, C2, R2	42.7138	70.4123	2263	0.607	1.0000
Loot, C2, R2 - Soldier, C2, R3	-395.8056	70.4123	2263	-5.621	<.0001
Loot, C2, R2 - Soldier, C2, R4	-1017.1810	70.4123	2263	-14.446	<.0001
Loot, C2, R3 - Loot, C2, R4	-590.0487	70.4123	2263	-8.380	<.0001
Loot, C2, R3 - Red and black, C1, R1	-149.8995	70.4123	2263	-2.129	0.9642
Loot, C2, R3 - Red and black, C1, R2	-644.2292	70.4123	2263	-9.149	<.0001
Loot, C2, R3 - Red and black, C1, R3	-880.7682	70.4123	2263	-12.509	<.0001
Loot, C2, R3 - Red and black, C1, R4	-908.4082	70.4123	2263	-12.901	<.0001
Loot, C2, R3 - Red and black, C2, R1	403.5626	70.4123	2263	5.731	<.0001
Loot, C2, R3 - Red and black, C2, R2	116.8738	70.4123	2263	1.660	0.9992
Loot, C2, R3 - Red and black, C2, R3	-299.3451	70.4123	2263	-4.251	0.0087
Loot, C2, R3 - Red and black, C2, R4	-640.5226	70.4123	2263	-9.097	<.0001
Loot, C2, R3 - Soldier, C1, R1	417.2887	70.4123	2263	5.926	<.0001
Loot, C2, R3 - Soldier, C1, R2	-192.1174	70.4123	2263	-2.728	0.6376
Loot, C2, R3 - Soldier, C1, R3	-624.4323	70.4123	2263	-8.868	<.0001
Loot, C2, R3 - Soldier, C1, R4	-815.6785	70.4123	2263	-11.584	<.0001
Loot, C2, R3 - Soldier, C2, R1	714.4174	70.4123	2263	10.146	<.0001
Loot, C2, R3 - Soldier, C2, R2	499.4564	70.4123	2263	7.093	<.0001
Loot, C2, R3 - Soldier, C2, R3	60.9369	70.4123	2263	0.865	1.0000
Loot, C2, R3 - Soldier, C2, R4	-560.4385	70.4123	2263	-7.959	<.0001
Loot, C2, R4 - Red and black, C1, R1	440.1492	70.4123	2263	6.251	<.0001
Loot, C2, R4 - Red and black, C1, R2	-54.1805	70.4123	2263	-0.769	1.0000
Loot, C2, R4 - Red and black, C1, R3	-290.7195	70.4123	2263	-4.129	0.0142
Loot, C2, R4 - Red and black, C1, R4	-318.3595	70.4123	2263	-4.521	0.0027
Loot, C2, R4 - Red and black, C2, R1	993.6113	70.4123	2263	14.111	<.0001
Loot, C2, R4 - Red and black, C2, R2	706.9226	70.4123	2263	10.040	<.0001
Loot, C2, R4 - Red and black, C2, R3	290.7036	70.4123	2263	4.129	0.0142
Loot, C2, R4 - Red and black, C2, R4	-50.4738	70.4123	2263	-0.717	1.0000
Loot, C2, R4 - Soldier, C1, R1	1007.3374	70.4123	2263	14.306	<.0001
Loot, C2, R4 - Soldier, C1, R2	397.9313	70.4123	2263	5.651	<.0001
Loot, C2, R4 - Soldier, C1, R3	-34.3836	70.4123	2263	-0.488	1.0000
Loot, C2, R4 - Soldier, C1, R4	-225.6297	70.4123	2263	-3.204	0.2684
Loot, C2, R4 - Soldier, C2, R1	1304.4662	70.4123	2263	18.526	<.0001
Loot, C2, R4 - Soldier, C2, R2	1089.5051	70.4123	2263	15.473	<.0001

Table 8 – *Continued from previous page*

contrast	estimate	SE	df	t.ratio	p.value
Loot, C2, R4 - Soldier, C2, R3	650.9856	70.4123	2263	9.245	<.0001
Loot, C2, R4 - Soldier, C2, R4	29.6103	70.4123	2263	0.421	1.0000
Red and black, C1, R1 - Red and black, C1, R2	-494.3297	70.4123	2263	-7.021	<.0001
Red and black, C1, R1 - Red and black, C1, R3	-730.8687	70.4123	2263	-10.380	<.0001
Red and black, C1, R1 - Red and black, C1, R4	-758.5087	70.4123	2263	-10.772	<.0001
Red and black, C1, R1 - Red and black, C2, R1	553.4621	70.4123	2263	7.860	<.0001
Red and black, C1, R1 - Red and black, C2, R2	266.7733	70.4123	2263	3.789	0.0494
Red and black, C1, R1 - Red and black, C2, R3	-149.4456	70.4123	2263	-2.122	0.9655
Red and black, C1, R1 - Red and black, C2, R4	-490.6231	70.4123	2263	-6.968	<.0001
Red and black, C1, R1 - Soldier, C1, R1	567.1882	70.4123	2263	8.055	<.0001
Red and black, C1, R1 - Soldier, C1, R2	-42.2179	70.4123	2263	-0.600	1.0000
Red and black, C1, R1 - Soldier, C1, R3	-474.5328	70.4123	2263	-6.739	<.0001
Red and black, C1, R1 - Soldier, C1, R4	-665.7790	70.4123	2263	-9.455	<.0001
Red and black, C1, R1 - Soldier, C2, R1	864.3169	70.4123	2263	12.275	<.0001
Red and black, C1, R1 - Soldier, C2, R2	649.3559	70.4123	2263	9.222	<.0001
Red and black, C1, R1 - Soldier, C2, R3	210.8364	70.4123	2263	2.994	0.4183
Red and black, C1, R1 - Soldier, C2, R4	-410.5390	70.4123	2263	-5.831	<.0001
Red and black, C1, R2 - Red and black, C1, R3	-236.5390	70.4123	2263	-3.359	0.1824
Red and black, C1, R2 - Red and black, C1, R4	-264.1790	70.4123	2263	-3.752	0.0560
Red and black, C1, R2 - Red and black, C2, R1	1047.7918	70.4123	2263	14.881	<.0001
Red and black, C1, R2 - Red and black, C2, R2	761.1031	70.4123	2263	10.809	<.0001
Red and black, C1, R2 - Red and black, C2, R3	344.8841	70.4123	2263	4.898	0.0005
Red and black, C1, R2 - Red and black, C2, R4	3.7067	70.4123	2263	0.053	1.0000
Red and black, C1, R2 - Soldier, C1, R1	1061.5179	70.4123	2263	15.076	<.0001
Red and black, C1, R2 - Soldier, C1, R2	452.1118	70.4123	2263	6.421	<.0001
Red and black, C1, R2 - Soldier, C1, R3	19.7969	70.4123	2263	0.281	1.0000
Red and black, C1, R2 - Soldier, C1, R4	-171.4492	70.4123	2263	-2.435	0.8474
Red and black, C1, R2 - Soldier, C2, R1	1358.6467	70.4123	2263	19.296	<.0001
Red and black, C1, R2 - Soldier, C2, R2	1143.6856	70.4123	2263	16.243	<.0001
Red and black, C1, R2 - Soldier, C2, R3	705.1662	70.4123	2263	10.015	<.0001
Red and black, C1, R2 - Soldier, C2, R4	83.7908	70.4123	2263	1.190	1.0000
Red and black, C1, R3 - Red and black, C1, R4	-27.6400	70.4123	2263	-0.393	1.0000
Red and black, C1, R3 - Red and black, C2, R1	1284.3308	70.4123	2263	18.240	<.0001
Red and black, C1, R3 - Red and black, C2, R2	997.6421	70.4123	2263	14.169	<.0001
Red and black, C1, R3 - Red and black, C2, R3	581.4231	70.4123	2263	8.257	<.0001
Red and black, C1, R3 - Red and black, C2, R4	240.2456	70.4123	2263	3.412	0.1582
Red and black, C1, R3 - Soldier, C1, R1	1298.0569	70.4123	2263	18.435	<.0001
Red and black, C1, R3 - Soldier, C1, R2	688.6508	70.4123	2263	9.780	<.0001
Red and black, C1, R3 - Soldier, C1, R3	256.3359	70.4123	2263	3.640	0.0804
Red and black, C1, R3 - Soldier, C1, R4	65.0897	70.4123	2263	0.924	1.0000
Red and black, C1, R3 - Soldier, C2, R1	1595.1856	70.4123	2263	22.655	<.0001
Red and black, C1, R3 - Soldier, C2, R2	1380.2246	70.4123	2263	19.602	<.0001
Red and black, C1, R3 - Soldier, C2, R3	941.7051	70.4123	2263	13.374	<.0001
Red and black, C1, R3 - Soldier, C2, R4	320.3297	70.4123	2263	4.549	0.0024
Red and black, C1, R4 - Red and black, C2, R1	1311.9708	70.4123	2263	18.633	<.0001
Red and black, C1, R4 - Red and black, C2, R2	1025.2821	70.4123	2263	14.561	<.0001
Red and black, C1, R4 - Red and black, C2, R3	609.0631	70.4123	2263	8.650	<.0001
Red and black, C1, R4 - Red and black, C2, R4	267.8856	70.4123	2263	3.805	0.0468
Red and black, C1, R4 - Soldier, C1, R1	1325.6969	70.4123	2263	18.828	<.0001
Red and black, C1, R4 - Soldier, C1, R2	716.2908	70.4123	2263	10.173	<.0001
Red and black, C1, R4 - Soldier, C1, R3	283.9759	70.4123	2263	4.033	0.0205

Table 8 – *Continued from previous page*

contrast	estimate	SE	df	t.ratio	p.value
Red and black, C1, R4 - Soldier, C1, R4	92.7297	70.4123	2263	1.317	1.0000
Red and black, C1, R4 - Soldier, C2, R1	1622.8256	70.4123	2263	23.047	<.0001
Red and black, C1, R4 - Soldier, C2, R2	1407.8646	70.4123	2263	19.995	<.0001
Red and black, C1, R4 - Soldier, C2, R3	969.3451	70.4123	2263	13.767	<.0001
Red and black, C1, R4 - Soldier, C2, R4	347.9697	70.4123	2263	4.942	0.0004
Red and black, C2, R1 - Red and black, C2, R2	-286.6887	70.4123	2263	-4.072	0.0177
Red and black, C2, R1 - Red and black, C2, R3	-702.9077	70.4123	2263	-9.983	<.0001
Red and black, C2, R1 - Red and black, C2, R4	-1044.0851	70.4123	2263	-14.828	<.0001
Red and black, C2, R1 - Soldier, C1, R1	13.7262	70.4123	2263	0.195	1.0000
Red and black, C2, R1 - Soldier, C1, R2	-595.6800	70.4123	2263	-8.460	<.0001
Red and black, C2, R1 - Soldier, C1, R3	-1027.9949	70.4123	2263	-14.600	<.0001
Red and black, C2, R1 - Soldier, C1, R4	-1219.2410	70.4123	2263	-17.316	<.0001
Red and black, C2, R1 - Soldier, C2, R1	310.8549	70.4123	2263	4.415	0.0044
Red and black, C2, R1 - Soldier, C2, R2	95.8938	70.4123	2263	1.362	1.0000
Red and black, C2, R1 - Soldier, C2, R3	-342.6256	70.4123	2263	-4.866	0.0006
Red and black, C2, R1 - Soldier, C2, R4	-964.0010	70.4123	2263	-13.691	<.0001
Red and black, C2, R2 - Red and black, C2, R3	-416.2190	70.4123	2263	-5.911	<.0001
Red and black, C2, R2 - Red and black, C2, R4	-757.3964	70.4123	2263	-10.757	<.0001
Red and black, C2, R2 - Soldier, C1, R1	300.4149	70.4123	2263	4.267	0.0081
Red and black, C2, R2 - Soldier, C1, R2	-308.9913	70.4123	2263	-4.388	0.0049
Red and black, C2, R2 - Soldier, C1, R3	-741.3062	70.4123	2263	-10.528	<.0001
Red and black, C2, R2 - Soldier, C1, R4	-932.5523	70.4123	2263	-13.244	<.0001
Red and black, C2, R2 - Soldier, C2, R1	597.5436	70.4123	2263	8.486	<.0001
Red and black, C2, R2 - Soldier, C2, R2	382.5826	70.4123	2263	5.433	<.0001
Red and black, C2, R2 - Soldier, C2, R3	-55.9369	70.4123	2263	-0.794	1.0000
Red and black, C2, R2 - Soldier, C2, R4	-677.3123	70.4123	2263	-9.619	<.0001
Red and black, C2, R3 - Red and black, C2, R4	-341.1774	70.4123	2263	-4.845	0.0006
Red and black, C2, R3 - Soldier, C1, R1	716.6338	70.4123	2263	10.178	<.0001
Red and black, C2, R3 - Soldier, C1, R2	107.2277	70.4123	2263	1.523	0.9999
Red and black, C2, R3 - Soldier, C1, R3	-325.0872	70.4123	2263	-4.617	0.0018
Red and black, C2, R3 - Soldier, C1, R4	-516.3333	70.4123	2263	-7.333	<.0001
Red and black, C2, R3 - Soldier, C2, R1	1013.7626	70.4123	2263	14.398	<.0001
Red and black, C2, R3 - Soldier, C2, R2	798.8015	70.4123	2263	11.345	<.0001
Red and black, C2, R3 - Soldier, C2, R3	360.2821	70.4123	2263	5.117	0.0002
Red and black, C2, R3 - Soldier, C2, R4	-261.0933	70.4123	2263	-3.708	0.0647
Red and black, C2, R4 - Soldier, C1, R1	1057.8113	70.4123	2263	15.023	<.0001
Red and black, C2, R4 - Soldier, C1, R2	448.4051	70.4123	2263	6.368	<.0001
Red and black, C2, R4 - Soldier, C1, R3	16.0903	70.4123	2263	0.229	1.0000
Red and black, C2, R4 - Soldier, C1, R4	-175.1559	70.4123	2263	-2.488	0.8158
Red and black, C2, R4 - Soldier, C2, R1	1354.9400	70.4123	2263	19.243	<.0001
Red and black, C2, R4 - Soldier, C2, R2	1139.9790	70.4123	2263	16.190	<.0001
Red and black, C2, R4 - Soldier, C2, R3	701.4595	70.4123	2263	9.962	<.0001
Red and black, C2, R4 - Soldier, C2, R4	80.0841	70.4123	2263	1.137	1.0000
Soldier, C1, R1 - Soldier, C1, R2	-609.4062	70.4123	2263	-8.655	<.0001
Soldier, C1, R1 - Soldier, C1, R3	-1041.7210	70.4123	2263	-14.795	<.0001
Soldier, C1, R1 - Soldier, C1, R4	-1232.9672	70.4123	2263	-17.511	<.0001
Soldier, C1, R1 - Soldier, C2, R1	297.1287	70.4123	2263	4.220	0.0099
Soldier, C1, R1 - Soldier, C2, R2	82.1677	70.4123	2263	1.167	1.0000
Soldier, C1, R1 - Soldier, C2, R3	-356.3518	70.4123	2263	-5.061	0.0002
Soldier, C1, R1 - Soldier, C2, R4	-977.7272	70.4123	2263	-13.886	<.0001
Soldier, C1, R2 - Soldier, C1, R3	-432.3149	70.4123	2263	-6.140	<.0001

Table 8 – *Continued from previous page*

contrast	estimate	SE	df	t.ratio	p.value
Soldier, C1, R2 - Soldier, C1, R4	-623.5610	70.4123	2263	-8.856	<.0001
Soldier, C1, R2 - Soldier, C2, R1	906.5349	70.4123	2263	12.875	<.0001
Soldier, C1, R2 - Soldier, C2, R2	691.5738	70.4123	2263	9.822	<.0001
Soldier, C1, R2 - Soldier, C2, R3	253.0544	70.4123	2263	3.594	0.0931
Soldier, C1, R2 - Soldier, C2, R4	-368.3210	70.4123	2263	-5.231	0.0001
Soldier, C1, R3 - Soldier, C1, R4	-191.2462	70.4123	2263	-2.716	0.6477
Soldier, C1, R3 - Soldier, C2, R1	1338.8497	70.4123	2263	19.014	<.0001
Soldier, C1, R3 - Soldier, C2, R2	1123.8887	70.4123	2263	15.962	<.0001
Soldier, C1, R3 - Soldier, C2, R3	685.3692	70.4123	2263	9.734	<.0001
Soldier, C1, R3 - Soldier, C2, R4	63.9938	70.4123	2263	0.909	1.0000
Soldier, C1, R4 - Soldier, C2, R1	1530.0959	70.4123	2263	21.731	<.0001
Soldier, C1, R4 - Soldier, C2, R2	1315.1349	70.4123	2263	18.678	<.0001
Soldier, C1, R4 - Soldier, C2, R3	876.6154	70.4123	2263	12.450	<.0001
Soldier, C1, R4 - Soldier, C2, R4	255.2400	70.4123	2263	3.625	0.0845
Soldier, C2, R1 - Soldier, C2, R2	-214.9610	70.4123	2263	-3.053	0.3731
Soldier, C2, R1 - Soldier, C2, R3	-653.4805	70.4123	2263	-9.281	<.0001
Soldier, C2, R1 - Soldier, C2, R4	-1274.8559	70.4123	2263	-18.106	<.0001
Soldier, C2, R2 - Soldier, C2, R3	-438.5195	70.4123	2263	-6.228	<.0001
Soldier, C2, R2 - Soldier, C2, R4	-1059.8949	70.4123	2263	-15.053	<.0001
Soldier, C2, R3 - Soldier, C2, R4	-621.3754	70.4123	2263	-8.825	<.0001

Results are averaged over the levels of: DoF

Degrees-of-freedom method: kenward-roger

P value adjustment: tukey method for comparing a family of 32 estimates

Table 9: Contrast test between factors DoF and Content

contrast	estimate	SE	df	t.ratio	p.value
C1, R1 - C1, R2	-263.7783	40.7258	2294	-6.477	<.0001
C1, R1 - C1, R3	-803.3192	40.7258	2294	-19.725	<.0001
C1, R1 - C1, R4	-962.2388	40.7258	2294	-23.627	<.0001
C1, R1 - C2, R1	281.7562	40.7258	2294	6.918	<.0001
C1, R1 - C2, R2	-140.8103	40.7258	2294	-3.458	0.0129
C1, R1 - C2, R3	-654.9223	40.7258	2294	-16.081	<.0001
C1, R1 - C2, R4	-925.6729	40.7258	2294	-22.729	<.0001
C1, R2 - C1, R3	-539.5409	40.7258	2294	-13.248	<.0001
C1, R2 - C1, R4	-698.4605	40.7258	2294	-17.150	<.0001
C1, R2 - C2, R1	545.5345	40.7258	2294	13.395	<.0001
C1, R2 - C2, R2	122.9681	40.7258	2294	3.019	0.0521
C1, R2 - C2, R3	-391.1440	40.7258	2294	-9.604	<.0001
C1, R2 - C2, R4	-661.8946	40.7258	2294	-16.252	<.0001
C1, R3 - C1, R4	-158.9196	40.7258	2294	-3.902	0.0025
C1, R3 - C2, R1	1085.0754	40.7258	2294	26.643	<.0001
C1, R3 - C2, R2	662.5090	40.7258	2294	16.268	<.0001
C1, R3 - C2, R3	148.3969	40.7258	2294	3.644	0.0067
C1, R3 - C2, R4	-122.3537	40.7258	2294	-3.004	0.0544
C1, R4 - C2, R1	1243.9950	40.7258	2294	30.546	<.0001
C1, R4 - C2, R2	821.4286	40.7258	2294	20.170	<.0001
C1, R4 - C2, R3	307.3165	40.7258	2294	7.546	<.0001
C1, R4 - C2, R4	36.5659	40.7258	2294	0.898	0.9863

Table 9 – *Continued from previous page*

contrast	estimate	SE	df	t.ratio	p.value
C2, R1 - C2, R2	-422.5664	40.7258	2294	-10.376	<.0001
C2, R1 - C2, R3	-936.6785	40.7258	2294	-23.000	<.0001
C2, R1 - C2, R4	-1207.4291	40.7258	2294	-29.648	<.0001
C2, R2 - C2, R3	-514.1121	40.7258	2294	-12.624	<.0001
C2, R2 - C2, R4	-784.8627	40.7258	2294	-19.272	<.0001
C2, R3 - C2, R4	-270.7506	40.7258	2294	-6.648	<.0001

Results are averaged over the levels of: DoF, Contents

Degrees-of-freedom method: kenward-roger

P value adjustment: tukey method for comparing a family of 8 estimates